Testing the limitations of artificial protein degradation kinetics using known-age massive Porites coral skeletons

(Article begins on next page)

07 August 2024

Testing the limitations of artificial protein degradation kinetics using known-age massive *Porites* coral skeletons

Abstract

High-temperature isothermal heating of biominerals has commonly been used to artificially accelerate protein degradation in order to extrapolate kinetic parameters to the lower temperatures experienced *in vivo* and in the burial environment. It is not easy to test the accuracy of these simulations due to the difficulty of finding samples of known age held at a known temperature. We compare protein degradation in the intra-crystalline organic matrix of heated (80 °C, 110 °C, and 140 °C) massive *Porites* sp. coral to that directly measured in the skeleton of colonies growing at ~26 °C and deposited over the last five centuries. This provides the opportunity to critically evaluate the underlying assumption that high-temperature experiments accurately mimic degradation processes and kinetics occurring in a 'naturally aged' biomineral. In all samples the intra-crystalline protein fraction was isolated and the L- and D- concentration of multiple amino acids measured using reverse-phase high-performance liquid chromatography (RP-HPLC). There was no evidence of a failure of the closed system in the high-temperature experiments (assessed by X-ray diffraction, thermogravimetric analyses and determination of leached amino acid concentration). We compared conventional methods for estimation of kinetic parameters with a new 'model-free' approach that makes no assumptions regarding the underlying kinetics of the system and uses numerical optimisation to estimate relative rate differences. The 'model-free' approach generally produced more reliable estimates of the observed rates of racemization in 'naturally aged' coral, although rates of hydrolysis (as estimated from the release of free amino acids) were usually over-estimated. In the amino acids for which we were able to examine both racemization and hydrolysis (aspartic acid/asparagine, glutamic acid/glutamine and alanine), it was clear that hydrolysis was less temperature sensitive than racemization, which may account for the differences in degradation patterns observed between the 'naturally aged' coral and high-temperature data. It is clearly important to estimate the individual temperature dependence of each of the parallel reactions.

Highlights

► We compare protein degradation in heated modern, and naturally aged *Porites* coral. ► Heating to 140 °C does not compromise the integrity of the closed-system. ► We use a new approach that fits relative rates to estimate temperature dependence. ► Protein degradation patterns change over the temperatures investigated (26–140 °C). ► We observe different temperature sensitivities for hydrolysis and racemization.

Keywords

1. Introduction

1.1. Amino acid racemization (AAR) and high-temperature experiments

The temperature-dependence of reactions is often exploited in controlled high-temperature experiments to explore processes occurring over geological time scales that would otherwise be too slow to observe. This approach has many advantages for the study of amino acid racemization (AAR), the inter-conversion of L-amino acids (which constitute protein in living organisms) into an equilibrium mixture of L- and D-amino acids after tissue death. In addition to being a time-dependent process (and therefore used in geochronology), AAR is also strongly temperature-dependent and so isothermal heating of biominerals has been used as a convenient method of artificially accelerating protein degradation reactions (e.g. Bada, 1972; Mitterer, 1975; Masters and Bada, 1977; Kriausakul and Mitterer, 1978; Kimber and Griffin, 1987; Goodfriend and Meyer, 1991; Miller et al., 1991; Miller et al., 1992; Miller et al., 2000; Roof, 1997; Manley et al., 2000; Kaufman, 2000; Kaufman, 2006 ; Clarke and Murray-wallace, 2006). In practice, these experiments typically involve heating samples isothermally at a minimum of three elevated temperatures, over a range of time-lengths, and determining the extent of racemization (D/L value) and in some studies, hydrolysis.

1.2. Kinetic models

The estimate of a reaction rate constant (k) is typically achieved by transforming D/L values so that they are linear with respect to time, thereby allowing quantification of k from the slope of the resulting regression line (see Clarke and Murray-Wallace, 2006, and references therein). When heated, free amino acid racemization conforms to reversible first-order kinetics (RFOK) (Bada, 1984 and references therein). Racemization of bound amino acids in the proteins of both fossil and (heated) modern biominerals, on the other hand, can deviate significantly from RFOK (see Clarke and Murray-Wallace, 2006, and references therein), a pattern that is particularly apparent at high D/L values, and for the rapidly racemizing amino acid aspartic acid (e.g. Goodfriend, 1991; Goodfriend and Meyer, 1991 ; Manley et al., 2000). Consequently, empirical-based transformations have become more commonly used to calculate an "effective" or "pseudo" rate constant (reviewed by Clarke and Murray-Wallace, 2006). Irrespective of the transformation used, the calculated rate or "pseudo" rate constant characterizes the "observed" racemization reaction, which in reality is influenced by a network of underlying reactions, including hydrolysis and decomposition reactions (such as decarboxylation, deamination or deamidation; e.g. Wehmiller et al., 1976; Goodfriend and Meyer, 1991 ; Collins and Riley, 2000). The Arrhenius relationship (Equation (1), Box 1) describes the relationship between temperature and the rate of a reaction. Using k values acquired experimentally at elevated temperatures, and providing certain assumptions are met as discussed below, the Arrhenius relationship can be applied to quantify the temperature-sensitivity of k. This subsequently enables an estimate of the rate of racemization at the lower environmental temperatures that fossils are naturally exposed to (Box 1). In some cases this method has been used to estimate absolute ages for fossil biominerals (see Equation (3), Box 1, e.g. Mitterer, 1975; Mitterer and Kriausakul, 1989; Brooks et al., 1990 ; Miller et al., 1991). By providing estimates of the temperature sensitivity (i.e. activation energy, E_a) of racemization, isothermal heating experiments also enable palaeotemperature estimations based on the D/L values of fossils of known age (e.g. Kaufman, 2003). It is worth noting however, that in all cases (including this study), when the value of k for the observed degradation reaction does not represent a "true" rate constant, the activation energy (as well as other Arrhenius parameters) derived using k, is considered an "apparent" or "effective" activation energy.

Box 1.
Kinetic experiments and the Arrhenius relationship.

The Arrhenius relationship can be used to determine how the rate of an ideal gas phase reaction is affected by temperature. The relationship is widely used to explore the temperature-dependence of reactions, many of which do not conform to this ideal behaviour.

The Arrhenius equation can be given as:
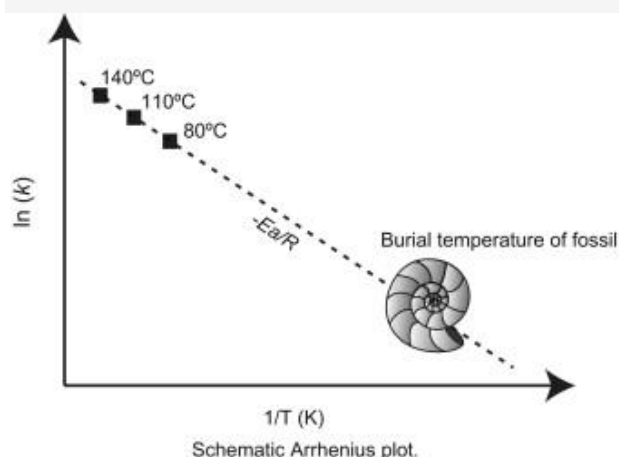
equation(1)

$$k = A\,e^{(-E_a/RT)}$$

k = the rate constant; A = the Pre-exponential factor (yr^{-1}); E_a = the activation energy (J mol^{-1}); R = the universal gas constant (8.314 J mol^{-1}); T = the absolute temperature (K). However, in order to calculate the temperature dependence of the rate constant, the two unknown parameters of the Arrhenius equation must be solved.

Equation (1) can be rearranged into "$y = mx + c$" form, to give:
equation(2)

$$\ln k = -E_a/RT + \ln(A)$$

In an "Arrhenius plot", the natural logarithm of the rate constant ($\ln k$) is plotted against the reciprocal of the absolute temperature in K ($1/T$).

Schematic Arrhenius plot.

If values of $\ln k$ acquired at 3 or more temperatures are plotted, according to equation(2), a straight line connecting these points will yield a slope (m) equal to $-E_a/R$, with a y-intercept of $\ln(A)$. The activation energy for the reaction is therefore equal to the gradient (m) × R.
It is therefore theoretically possible to determine k at any temperature, by substituting the values for E_a and A, and the desired temperature, into equation (1) (shown graphically in the schematic Arrhenius plot). Therefore, the rate constant for racemization can be calculated for a fossil, if its effective burial temperature (the integrated effect of all temperatures to which the fossil sample has been exposed (Wehmiller, 1977)) is known. The rate constant can subsequently be substituted into an appropriate 'age equation' to estimates the fossil's age; for example, if the rate constants are derived assuming reversible first order kinetics (RFOK) the following equation can be applied:
equation(3)

$$t = \frac{\ln\{(1 + D/L)/(1 - D/L)\} - \text{constant}}{2k}$$

constant = racemization induced during sample preparation; t = age of the sample (yrs); D/L = ratio of D to L enantiomers

There are several theoretical issues associated with extrapolating from high to low temperatures that may affect the validity of this approach (Kimber and Griffin, 1987; Goodfriend and Meyer, 1991; Walton, 1998; Collins et al., 1999; Collins and Riley, 2000 ; Demarchi et al., 2013a). Firstly, the use of kinetic models that do not adequately represent the observed reaction will result in inaccuracies in the derived rate constant and Arrhenius parameters (Goodfriend and Meyer, 1991). Secondly, fundamental to these experiments is the assumption that when heated, the protein fraction follows the same degradation pathways occurring under "normal" burial temperatures. This in turn relies on the assumption that either (i) the temperature sensitivities (the activation energies) of the parallel reactions contributing to k do not differ significantly, or, (ii) that these underlying reactions are inconsequential in determining the rate of racemization. If these assumptions are true, the line connecting the k values estimated at different temperatures on an Arrhenius plot (Box 1) should be linear. However, if the temperature-sensitivity of each reaction contributing to k varies, then these underlying reactions will influence k differently at higher temperatures. A limited number of studies utilizing different biominerals have sought to test these assumptions, with varying results (e.g.Goodfriend and Meyer, 1991; Miller et al., 2000; Laabs and Kaufman, 2003 ; Demarchi et al., 2013a).

A "hybrid" approach is often adopted to provide more robust estimates of the temperature-sensitivity of racemization that constrains data acquired during the high-temperature isothermal experiments using rates calculated in independently dated (unheated) fossils with estimated effective burial temperatures (e.g. see Miller et al., 1992; Manley et al., 2000 ; Kaufman, 2000). The uncertainty associated with extrapolations from high to ambient temperature is significantly reduced when using this hybrid approach, but even where appropriate fossil time-series are available for calibration, extracting accurate racemization data can still be problematic. In reality, rather than remaining at a constant temperature, fossil samples have usually experienced significant thermal fluctuations, particularly if both glacial and inter-glacial periods are included in the time range (see McCoy, 1987; Miller et al., 1999 ; Wehmiller and Miller, 2000). Furthermore, samples from archaeological sites may have been cooked or heated when buried close to a hearth (e.g. Masters and Bada, 1978). Finally, any error in independent age estimates will also contribute errors in subsequent calculations of racemization rates.

In this study we evaluate the underlying assumption that high-temperature experiments accurately mimic degradation processes and kinetics occurring in a 'naturally aged' biomineral exposed to environmental temperatures. In addition, we critically examine models used to derive estimates of the rate and temperature sensitivity of protein degradation reactions. Direct comparison between 'real-world' samples and the controlled conditions and constant temperatures of laboratory experiments is rarely achievable. Here we take advantage of exceptionally well-dated, massive aragonite skeletons deposited over centuries by tropical coral colonies of *Porites* sp. These colonies have grown in relatively stable sea-water temperatures of just above 26 °C (Hendy et al., 2002) and are accurately dated (Hendy et al., 2003). The skeleton of these corals contains a protein-rich "organic matrix" (OM) that constitutes ~1% of the dry weight (Cuif et al., 2004). We compare protein degradation pathways in skeleton from a modern *Porites* colony heated to 80 °C, 110 °C, or 140 °C, with protein degradation occurring in 'naturally aged' skeleton deposited over the last five centuries. We focus particularly on the degradation of the acidic amino acid aspartic acid that dominates the OM protein of corals (Young, 1971; Mitterer, 1978; Constantz and Weiner, 1988; Goodfriend et al., 1992; Cuif et al., 1999; Ingalls et al., 2003; Puverel et al., 2005 ; Hendy et al., 2012), and is well-known for its relatively fast racemization in carbonate fossils (Goodfriend, 1992).

2. Materials and methods

2.1. Massive *Porites* coral core samples

The 'naturally aged' coral samples examined in this study come from seven 2–5 m long cores drilled from living massive *Porites* sp. colonies. The actively calcifying live coral tissue is a ~10 mm thick surface layer, covering an aragonitic skeleton (a metastable polymorph of calcium carbonate) that has continuously accumulated at ~1–2 cm/year over a multi-century lifetime to form massive colonies. Calcification occurs extracellular but under strictly controlled conditions (e.g. Mass et al., 2011) beneath the calicoblastic tissue, isolated from seawater by two layers of tissue and the coelenteron. Since the skeleton cores come from living colonies it would be incorrect to refer to the samples as 'fossils'; instead we refer to them as 'naturally aged' to distinguish them from the experimentally heated samples.

The sampled colonies are from inshore and mid-shelf reefs in the central Great Barrier Reef (GBR), Australia, and Jarvis Island in the central equatorial Pacific (Table 1; Fig. 1 detailed in Hendy et al., 2012). The Great Barrier Reef cores were independently dated in a previous study (Hendy et al., 2003) using a combination of annual density banding from X-radiographs and cross-dating using characteristic patterns of annual luminescent lines evident under UV light. Typical errors found for coral core age estimates from annual banding are 1–2 years/century (Hendy et al., 2003). Together, the seven GBR cores span ~422 years of colony growth (Table 1). For the Jarvis coral, samples were analysed from three periods (1997, 1923 and 1858 AD) from a chronology established using a combination of seasonal and ENSO-related variations in monthly resolved skeletal $\delta^{18}O$ records, and annual skeletal density banding (Hendy et al., 2012). Due to the robust nature of these independent dating methods, any differences in AAR between coral cores are unlikely to be caused by mis-assignment of sample age. All colonies sampled in this study grew within a narrow temperature range (see Table 1).

Table 1.
Site details for the eight massive *Porites* sp. coral cores used in this study. Mean annual SST from the NOAA NCEP EMC CMB GLOBAL Ov2 climatology for 1961–1990 (Reynolds et al., 2002).

Coral locality	Latitude (°S)	Longitude (°E)	Distance from continental land mass (km)	Earliest date analysed in core (age in yrs)	Mean annual SST (°C)
Central Equatorial Pacific					
Jarvis Is.	0.37	200.02	>1000	1858 (141)	27.1
Central Great Barrier Reef					
Kurrimine Rf.	17.78	146.13	0 (inshore)	1850 (138)	26.4
Brook Is.	18.09	146.17	29 (inshore)	1755 (232)	26.2
Britomart Rf. a	18.14	146.44	36 (midshelf)	1740 (244)	26.2
Britomart Rf. b				1565 (422)	
Lodestone Rf.	18.42	147.06	70 (midshelf)	1850 (134)	26.1
Pandora Rf.	18.82	146.43	16 (inshore)	1735 (249)	26.2
Havannah Is.	18.85	146.55	24 (inshore)	1680 (308)	26.2
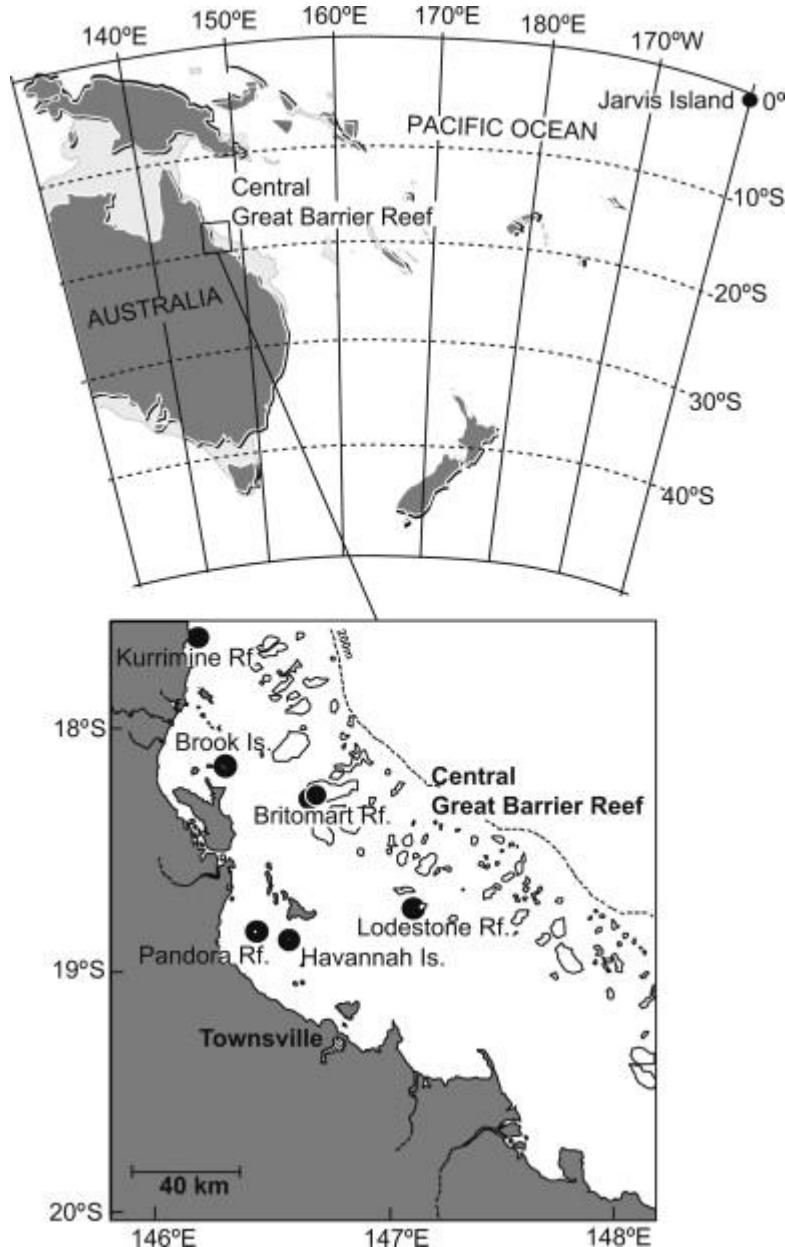
Fig. 1. Massive *Porites* sp. coral core sample sites.

Core slices were subjected to repeated and focused ultrasonic cleaning in high-purity (18 MΩ) Milli-Q water, and dried at <40 °C for a maximum of 48 h. Skeletal material was milled from along the centre of a growth axis to produce a fine powder. Duplicates for the same time period were collected from adjacent growth axes. The majority of samples contain a 5-year increment of skeletal growth. The "modern" coral material used for the isothermal heating experiments was deposited by the Jarvis Island colony in 1999; the same bulk sample was used in all the heating experiments. Therefore, while the 'naturally aged' samples (although treated here as a single system) were collected from different colonies, and show some between-colony variation (see Hendy et al., 2012 for further details), all the heated coral samples originated from the same colony.

2.2. Isolating the intra-crystalline fraction

Protein degradation is simpler to study within a closed-system (Towe, 1980; Sykes et al., 1995 ; Collins and Riley, 2000). Exposure of skeletal material to a strong chemical oxidant (such as bleach) isolates a 'protected' component of the organic matrix, referred to as the 'intra-crystalline fraction' (Towe, 1980 ; Berman et al., 1993). This intra-crystalline fraction has been shown to effectively operate as a closed system in a range of biominerals (Penkman et al., 2008a; Penkman et al., 2011; Demarchi et al., 2011; Demarchi et al., 2013a ; Crisp et al., 2013), although not within the freshwater bivalves *Margaritifera falcata* (Orem and Kaufman, 2011) and *Corbicula* (Penkman et al., 2007). The protocol used to isolate the intra-crystalline fraction in our samples follows Hendy et al. (2012); all powdered coral samples (both 'naturally aged' and modern) were exposed to 12% NaOCl (50 μL/mg of sample) for 48 h, maximizing removal of the inter-crystalline proteins but minimizing bleach-induced racemization. Following removal of the bleach, the powdered material is rinsed thoroughly (5 times and centrifuged between rinses) with ultrapure Milli-Q water, with a final methanol rinse.

2.3. Isothermal heating experiments

The coral skeletal powder was heated under aqueous conditions (Fig. 2). This provides a similar degradation environment to that experienced by the 'naturally aged' coral and in addition, enables us to test the integrity of the closed system by monitoring for loss of amino acids from the biomineral system (e.g. Penkman et al., 2008a; see Section 2.4). The results reported by Hendy et al. (2012) suggest that AAR within the intra-crystalline fraction of *Porites* sp. coral does follow closed-system behaviour. Exposure to high temperatures may, however, result in mineralogical and micro-structural changes (e.g.Epstein et al., 1953; Land et al., 1975; Dunbar and Wellington, 1981 ; Gaffey, 1988). The influence of such changes on the integrity of the closed system for amino acids has not been previously examined.
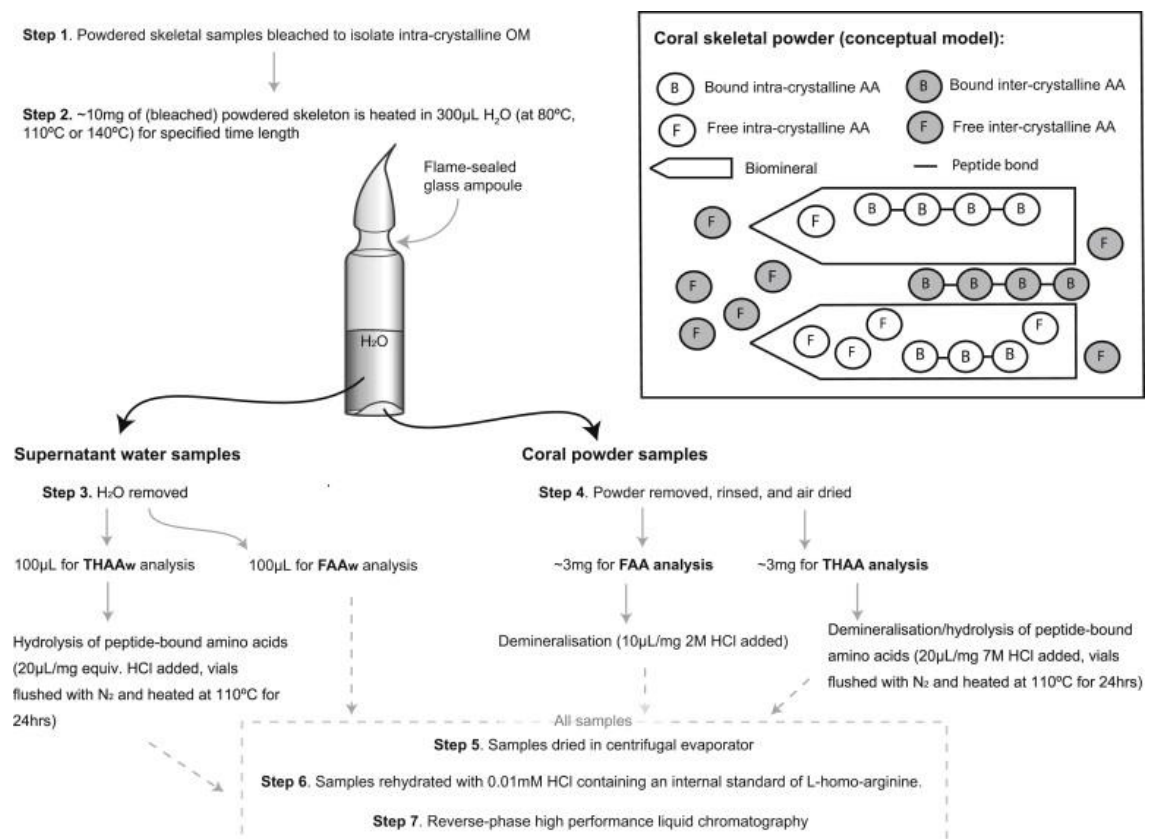

Fig. 2.

The methods used to heat samples in this study are outlined in Fig. 2. Between 8 and 10 mg of the bleached modern coral powder was weighed into sterile glass ampoules. 300 µL of ultrapure (18 MΩ) water was subsequently added to each ampoule before it was flame-sealed. Samples were placed in an oven maintained at a constant temperature of either 80 °C, 110 °C or 140 °C, for specified time-lengths, ranging from 24 to 5760 h (see Tables A1 and A2 of the supplementary material). For each of the designated time-lengths, 2 or more replicates were prepared. Experimental water blanks (300 µL of ultrapure water without coral powder) were prepared and treated in the same manner.

It should be noted that the heating experiments were conducted on material that had been bleached prior to diagenesis, while in the case of the 'naturally aged' coral, bleaching occurred post-diagenesis. Given that protein degradation in the intra-crystalline fraction effectively operates as a closed-system in *Porites* coral (Hendy et al., 2012), this should not impact the results. In addition, skeletal material from a *Porites* colony at Pandora reef (Table 1) was bleach-treated post heating to confirm that there was no significant difference resulting from the timing of bleach treatment relative to heating (see Section 3.2 for further discussion).

2.4. Amino acid analyses

Each of the (i) bleached 'naturally aged' coral powder samples, (ii) bleached experimentally heated powder samples, and (iii) supernatant water samples, were prepared for analysis following the protocol of Penkman et al. (2008a). Proteins must be broken down into their constituent amino acids prior to RP-HPLC analysis, a process that also occurs spontaneously over time through peptide bond hydrolysis. Degraded samples can be analysed for naturally hydrolysed (free) amino acids, whereas a measure of all amino acids (total) requires that the remaining peptide bonds are hydrolysed, typically by concentrated mineral acid at high temperature. Analysis of bleached samples with and without this additional hydrolysis step gives two alternative measurements of the composition of the amino acid: the Free Amino Acid (FAA) fraction and the Total Hydrolysable Amino Acid (THAA) fraction. Examining both THAA and FAA fractions reveals further aspects of protein degradation, in addition to the extent of racemization of each amino acid.

To detect any leaching of amino acids from the intra-crystalline fraction, 100 µL of supernatant water was removed for analysis of the free amino acid fraction ("FAAw") and 100 µL was removed for analysis of the total hydrolysable amino acid fraction ("THAAw"). The coral skeletal powder was air-dried and two sub-samples (each of ~3 mg) were weighed out for the analysis of the "FAA" and "THAA" fraction (see Fig. 2).

RP-HPLC analysis was performed using fluorescence detection, following a modified method of Kaufman and Manley (1998). The concentration of L and D enantiomers of 10 amino acids were analysed routinely. It is not possible to distinguish between the acidic amino acids and their amine derivatives because both asparagine and glutamine undergo rapid irreversible deamination during preparative hydrolysis to aspartic acid and glutamic acid respectively (Hill, 1965). Aspartic acid and asparagine are therefore reported together as Asx, and glutamic acid and glutamine as Glx.

2.4.1. Data screening

Data screening was applied with the aim of identifying data points that clearly indicate compromised samples, while retaining the natural variability of the data set. Two data screening methods were used. The first was applied to examine disparity between replicates. Secondly, a series of regression-based statistical data-screening tests (based on the methods of Kosnik and Kaufman, 2008 ; Hendy et al., 2012) were applied to the heated coral powder data set to identify outlying data points (see Figs. A1 and A2 and additional information in the supplementary material for further details regarding the methods used here). However, the regression-based screening tests are most robust when applied to large sample population sizes, as is the case for the 'naturally aged' data set. Therefore, when applying these tests to the experimental data, unlike in Hendy et al. (2012), data-points were not automatically excluded if identified as outliers. They were only rejected if, when examined in close detail, other discrepancies such as anomalously high/low concentrations were identified, or if they were highlighted by the replicate disparity test. The replicate disparity-screening test resulted in the exclusion of 3 out of 95 THAAw data-points, and 1 out of 99 FAAw data-points. For the heat-treated coral powder samples, replicate disparity and regression-based screening tests results in the exclusion of 7 out of 101 THAA data-points, and 7 out of 96 FAA data-points.

2.5. Mineralogical tests

Ampoules with "modern" coral powder were also heated under identical conditions for mineralogical characterization. Samples of both bleached powder (exposed to NaOCl) and non-bleached powder (i.e. samples containing both intra- and inter-crystalline OM fractions) were heated for a variety of time-lengths at 80 °C, 110 °C and 140 °C. X-ray diffraction (XRD) was used to determine the mineralogy of these samples before and after the isothermal heating experiments. Dry powders were mounted onto silicon wafer discs and data collected in the range $20° < 2\vartheta < 70°$ on a Bruker-AXS D8 Advance Power Diffractometer (Cu-K_α radiation; 1.5418Å, and a PSD LynxEye detector). Diffraction data was processed and evaluated using DIFFRACplus EVA analysis software, in conjunction with data from the International Centre for Diffraction Data (ICDD) database. Anhydrous crystalline polymorphs of calcium carbonate all produce characteristic diffraction patterns (ICDD PDF: 41-1475 [aragonite]; 5-586 [calcite]; 33-268 [vaterite]), enabling their identification.

Thermogravimetric analyses were carried out on previously unheated bleached and unbleached powder samples to examine the thermal decomposition of *Porites* skeleton. Samples were heated to 1000 °C at 10 °C/min, in order to determine the change in mass over time, as a function of temperature. Analyses were performed using a Netzsch STA 409EP instrument.

3. Results and discussion

3.1. Amino acid composition of the organic matrix in *Porites* coral

Aspartic acid is the most abundant amino acid in the intra-crystalline organic matrix of *Porites* coral (48%), while glutamic acid is also found in relatively high concentrations (8%; Fig. 3). These two acidic amino acids have been found to dominate the OM of corals in all studies carried out to date (Young, 1971; Mitterer, 1978; Constantz and Weiner, 1988; Goodfriend et al., 1992; Cuif et al., 1999; Ingalls et al., 2003; Puverel et al., 2005 ; Hendy et al., 2012). High aspartic acid content is also characteristic of the skeleton of many other calcifying organisms, including molluscs (e.g. Weiner, 1979; Gotliv et al., 2003 ; Demarchi et al., 2013b), foraminifera (King and Hare, 1972), Alcyonarian corals (Rahman and Oomori, 2008) and ostracodes (Kaufman, 2000).
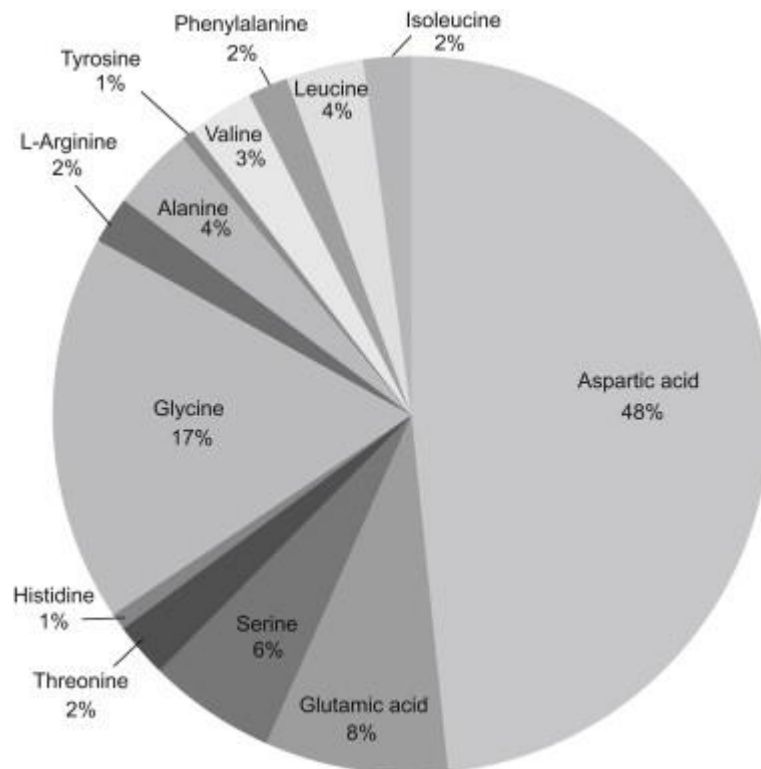
Fig. 3.
Average amino acid composition (*n* = 3) of the intra-crystalline organic matrix of unheated massive *Porites sp*. coral (from the 1999 Jarvis colony). As reported by other studies (e.g. Cuif et al., 1999), glycine represents a significant component of coral OM. However, the glycine peak produced following RP-HPLC is often poorly resolved (due to co-elution), causing considerable variation in estimates of OM glycine concentration between samples.

Following heating, the amino acid composition of the intra-crystalline OM changes significantly. Decomposition of amino acids can produce organic molecules, such as fumaric acid and ammonia from reversible deamination of aspartic acid (e.g. Bada and Miller, 1968 ; Bada and Miller, 1970), or other amino acids (e.g. serine dehydration to alanine, and decarboxylation of aspartic acid to alanine; see Vallentyne, 1964 ; Walton, 1998 and references therein for details). In addition to decomposition, free amino acids may also be lost following condensation with sugars (e.g. Hoering, 1973; Rafalska et al., 1991 ; Collins et al., 1992). These processes will alter the relative proportions of different amino acids in the OM of heat-induced as well as "naturally" degraded samples. If the respective temperature dependence of each of these reactions varies, their relative importance will also change at different temperatures.

3.2. Impact of heating on closed-system dynamics: leaching and skeletal mineralogy

After heating the coral powder, amino acid concentrations in the supernatant water remain low and within the analytical limit of detection (Fig. 4 and Fig. A3 in supplementary material), indicating that the carbonate skeleton remains effectively closed at the temperatures and time scales tested.
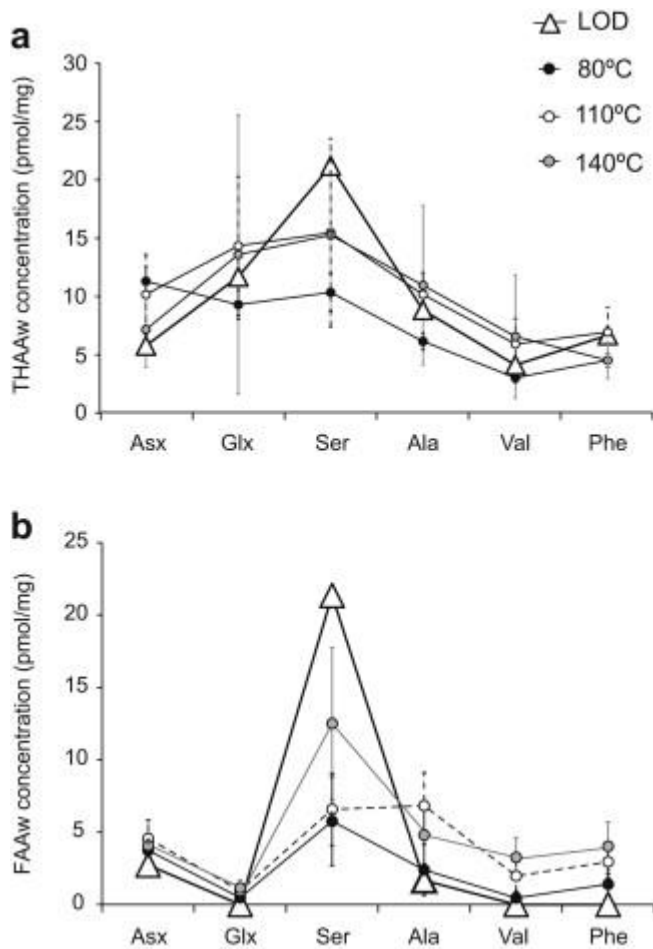
Fig. 4.
Average (a) THAAw and (b) FAAw concentrations of 6 amino acids in the supernatant water following heating of *Porites* coral at 80 °C, 110 °C and 140 °C. In both (a) and (b) the "Limit of detection" (LOD) was calculated as the LOD = X_{blank} + (3 * σ_{blank}); where X_{blank} is the mean of the blank measures, σ_{blank} is the standard deviations of the blank measures (n = 11). Error bars for the supernatant water concentrations (black = 80 °C, dashed = 110 °C, grey = 140 °C) represent ± 2 S.E. (standard error) about the mean value.

It is important to study the effects of heating on the biomineral as well as the proteins (Walton, 1998), as any change in crystal structure could compromise the behaviour of the intra-crystalline fraction. We confirmed that polymorph transition from aragonite to calcite was not induced by heating at the temperatures and over the time scales used in our experiments, for either the bleached or unbleached samples. Even after isothermal heating at 140 °C for the maximum time period studied (96 h), there was no evidence of phase conversion to calcite (Fig. 5a).
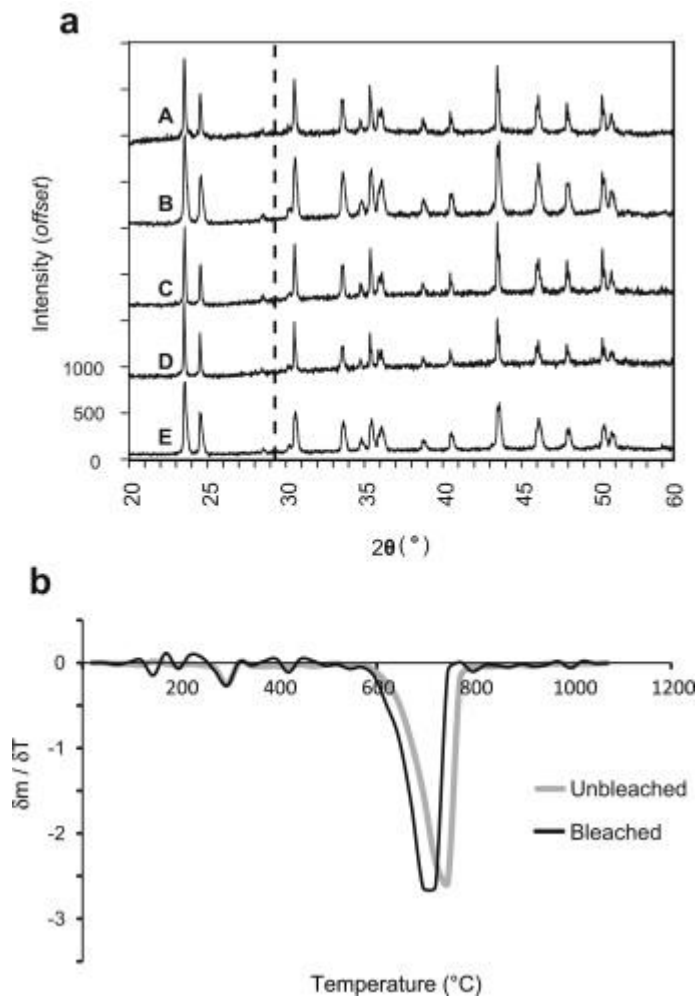
Fig. 5.
(a) Results of X-ray diffraction analyses for *Porites* coral powder. All peaks correspond to aragonite, with no calcite peaks present. A = bleached but unheated powder, B = unbleached unheated powder, C = bleached powder heated at 80 °C for 696 h, D = bleached powder heated at 110 °C for 696 h, E = bleached powder heated at 140 °C for 48 h. The dashed line indicates where the most intense peak for calcite would be expected to occur (2-theta = 29.1; D-spacing = 3.035 Å). The intensity scale is shown for the lowest spectra (sample E), but the additional spectra (samples A–D) are systematically offset from each other. (b) Differential thermogravimetric (DTG) plot derived from thermogravimetric analyses. The differential of mass (m = mW/mg) divided by the differential of time (T), is plotted against temperature (°C). The largest change in mass, occurring at ~600 °C is observed in the bleached skeleton (black line) before the unbleached skeleton (grey line).

TGA data (Fig. 5b) shows a weight loss at 270 °C associated with the loss of organic matrix and associated water. The bleached sample shows less weight loss (~2 wt%) than the unbleached sample (~3 wt%), as expected given their relative concentration of organic material. These values are comparable to previous studies (e.g. Cuif et al., 2004). Given that we observed decomposition at 270 °C, and this is known to occur at temperatures below that which cause phase conversion of aragonite to calcite (e.g. Mansur et al., 2005), we would expect phase purity to be maintained for all samples at the temperatures used for the artificial degradation experiments (<140 °C). Finally TGA reveals that the onset of decarboxylation occurs at about the same temperature (~570 °C) for both bleached and unbleached powder. However, we note that decomposition of the bleached material occurs more rapidly, being complete by ~745 °C, than is true of the unbleached material (complete by 770 °C) (Fig. 5b). Whilst beyond the scope of this study, further analysis of the powder processing conditions on the susceptibility to rapid thermal decomposition

(forming calcium oxide) at very high temperatures is advisable. The remaining sample has a residual mass of 53 wt%, for both the bleached and unbleached samples.

In this study, the heat-treated corals were bleached *prior* to heating (so that we could monitor the integrity of the closed-system upon heating), whereas in the 'naturally aged' corals, bleaching occurred *after* degradation. We recognise that this pre-treatment modifies the starting conditions of the artificial diagenesis experiments, and, in turn, could potentially account for differences in degradation patterns (Section 3.6). Bleach-induced changes to the biomineral are, however, unlikely to have compromised the integrity of the closed-system in the *Porites* samples because previous studies examining the effects of NaOCl on calcium carbonate dissolution have not observed significant impacts on the mineral (e.g. Pingitore et al., 1993 ; Gaffey and Bronnimann, 1993). In addition, we did not detect leaching of amino acids into the water that would indicate a breakdown in closed-system behaviour. The only difference between the bleached and unbleached samples observed in all our mineralogical analyses occurred >550 °C, far above the range of temperatures used to examine protein degradation (80–140 °C).

As a final confirmation that there was no significant impact caused by the timing of bleach treatment, we followed the method described in Section 2.3, with the exception of pre-bleaching, and heated (80 °C) aliquots of untreated coral powder (*Porites* skeleton collected from Pandora reef; Table 1). These samples were subsequently bleached after heating was complete. The results demonstrate that the pattern of degradation is consistent, whether the timing of bleach treatment is before or after heating (full comparison in Fig. A4 of the supplementary material). Therefore, although we suggest that the effects of pre-treatment with NaOCl on any biominerals used in AAR warrants further attention, we think it improbable that the results observed here are a consequence of differences in the timing of bleaching relative to protein degradation.

3.3. Racemization in *Porites coral*

The extent of amino acid racemization is much higher in the FAA fraction (consisting of free amino acids) than in the THAA fraction (which include free, internally bound, and terminally bound amino acids), as documented previously in both whole biomineral (e.g. Wehmiller and Hare, 1971; Kvenvolden et al., 1973 ; Miller and Brigham-Grette, 1989) and intra-crystalline studies (e.g. Penkman et al., 2007; Penkman et al., 2010; Penkman et al., 2011 ; Demarchi et al., 2011) (Fig. 6, supplementary material Fig. A5). The higher extent of FAA racemization is unlikely to be a result of increased rates of AAR when in the free form; it is more likely a consequence of the free amino acids having been formed via hydrolysis of already highly racemized amino acids (e.g. Kriausakul and Mitterer, 1978 ; Mitterer and Kriausakul, 1984). Racemization of bound amino acids has been hypothesised to occur more rapidly at the N-terminal position (Kriausakul and Mitterer, 1978; Kriausakul and Mitterer, 1980 ; Moir and Crawford, 1988), due to electron withdrawal increasing the ease of abstraction of the hydrogen from the α-carbon (Smith and Reddy, 1989). Racemization of internally bound amino acids is believed to be limited, as demonstrated by the very low D/L values found in high-molecular weight fractions of proteins in a variety of biominerals (e.g. Kimber and Griffin, 1987; Kimber and Hare, 1992; Kaufman and Miller, 1995 ; Kaufman and Sejrup, 1995). However for Asx (Geiger and Clarke, 1987) and probably serine (Takahashi et al., 2010) racemization is accelerated in chain, therefore contributing to the initially rapid rates of THAA racemization relative to other amino acids (e.g. Goodfriend, 1992; Goodfriend et al., 1992 ; Collins et al., 1999).
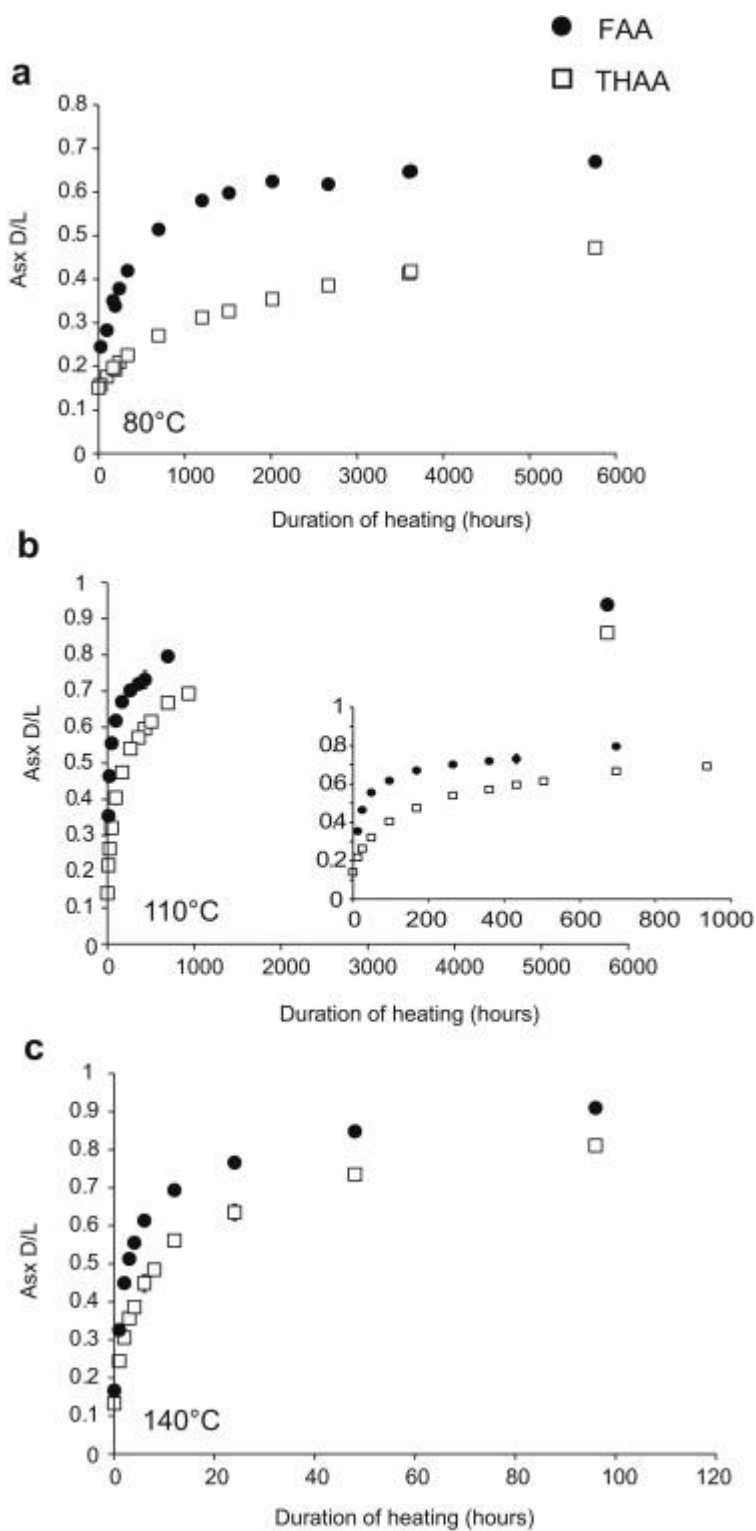
Fig. 6.
Asx racemization induced by isothermal heating experiments conducted at (a) 80 °C, (b) 110 °C (with data re-plotted in inset graph with shortened *x*-axis), and (c) 140 °C; Circles represent the mean FAA D/L, and squares the mean THAA D/L, for samples heated for the same duration. Error bars represent ± 2 S.E. about the mean. On occasions where only a single replicate was available, the value of the error bar was calculated as the mean value of all error bars at that temperature. This also applies for error bars plotted in Fig. 7, Fig. 8, Fig. 9, Fig. 10 ; Fig. 12.

When the extent of FAA and THAA Asx racemization at 80 °C, 110 °C and 140 °C is plotted together against heating time (Fig. 7a and b), the effect of increasing temperature on the rate of racemization is evident. In the FAA fraction, D/L values of above 0.6 are achieved after just ~6 h when coral powder is heated at 140 °C, while such levels of racemization are only reached in the 'naturally aged' *Porites* after ~200 years (~1.7×10^6 h). As in the heated samples, the extent of Asx racemization in the 'naturally aged' *Porites* is much higher in the FAA fraction than in the THAA (Fig. 7c). D/L vs heating time plots for other amino acids are provided in the supplementary material (Figs. A5–A7).
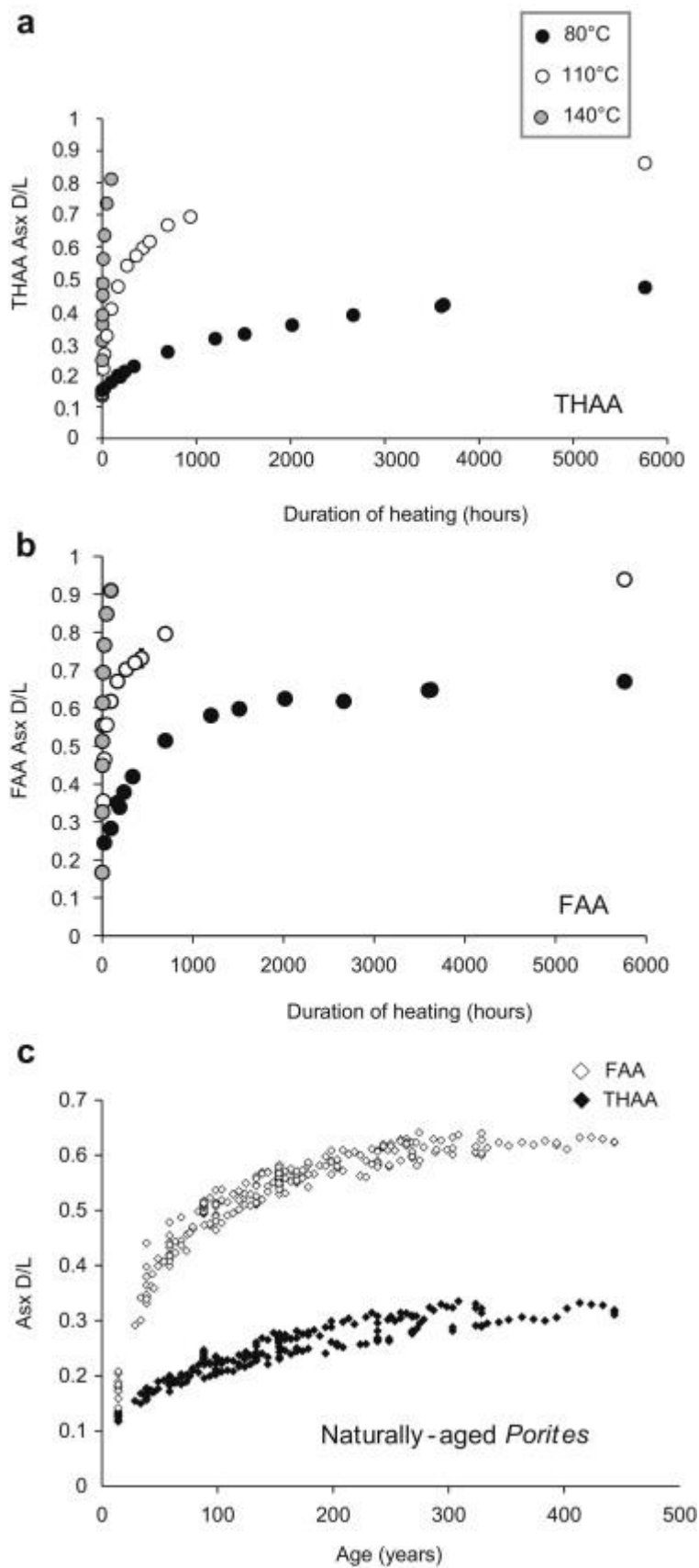
Fig. 7.
Graphs (a) and (b) show the effect of temperature on the extent of Asx racemization for the THAA and FAA fractions respectively (black circles = 80 °C, white circles = 110 °C, grey circles = 140 °C). Each data-point represents the mean of the samples heated for the same duration at the specified temperature. Error bars ± 2 S.E. about the mean value. Graph (c) shows the extent of Asx racemization with time in 'naturally

aged' *Porites* from the 8 different *Porites* coral cores (see Table 1). Black diamonds represent THAA data, and white diamonds, FAA data. Each data-point represents the mean of 2 analytical replicates.

### 3.4. Free amino acids in *Porites* coral

Hydrolysis acts to break peptide-bonds, creating shorter peptides, and eventually liberating free amino acids (e.g. see Wehmiller, 1980; Mitterer and Kriausakul, 1984; Bada, 1991 ; Collins and Riley, 2000). The rate of hydrolysis depends on temperature, the availability of water, and both the primary and higher order structure of proteins (e.g. Hill, 1965; Kriausakul and Mitterer, 1978; Bada, 1991; Collins et al., 1998; Walton, 1998 ; Collins and Riley, 2000 and references therein). Consequently as with racemization, taxonomic differences in rates of hydrolysis can be expected; indeed differences in the former are usually assumed to be a consequence of the latter. An example of a practical application of estimating hydrolysis patterns at high temperatures was presented by Miller et al. (1992). By measuring the concentration of both the free and total leucine (Leu) fraction in ostrich eggshell, Miller and colleagues were able to examine the patterns of Leu hydrolysis at a range of temperatures, which were described using a non-linear mathematical model. They estimated that the temperature sensitivity of Leu hydrolysis was ~10% lower than that of isoleucine (Ile) epimerization, and therefore the Ile epimerization value should increase more rapidly relative to the extent of Leu hydrolysis at higher temperatures; this information was then used to successfully distinguish between burned eggshell and those reworked from deeper levels at African archaeological sites.

The rate of hydrolysis can be monitored by observing the release of FAA, although this has not been reported in all kinetic studies, possibly due to issues of diffusive loss (see Roof, 1997) and leaching from open-system diagenetic environments. However, even in a closed-system, the rate of hydrolysis is likely to be underestimated due to subsequent decomposition of the FAA. The percentage of free amino acids (%FAA) is therefore used as a proxy for the rate of hydrolysis (and release of FAA):

equation(4)

$$\%FAA = ([FAA]/[THAA]) \times 100$$

[FAA] = Free amino acid concentration; [THAA] = Total hydrolysable amino acid concentration.

The 'naturally aged' *Porites* (~26 °C) examined in this study took between 120 and 200 years to reach %FAA Asx values of 10%. Equivalent levels of %FAA Asx were accrued after ~1200 h at 80 °C, ~80 h at 110 °C, and ~5 h at 140 °C. As the %FAA actually represents the liberation of FAA (hydrolysis) *minus* FAA lost by decomposition, if decomposition and hydrolysis reactions have significantly different temperature dependence, then this limits the use of %FAA as a proxy for hydrolysis when extrapolating from high temperature experiments. For example, the deamination of free aspartic acid in buffered solution (E_a 154 kJ mol^{-1} at pH 7; Bada and Miller, 1970) has a greater temperature sensitivity than hydrolysis of the Gly–Gly peptide bond in dipeptides (~44 kJ mol^{-1} at 265 atm or ~99 kJ mol^{-1} at water steam pressure; Qian et al., 1993). If hydrolysis of peptide bonds involving Asx has a similar temperature sensitivity to the Gly dipeptide, accelerated high-temperature decomposition of Asp would lower the %FAA and underestimate the rate of hydrolysis.

In both the heated and the 'naturally aged' coral, greater variability is generally observed in %FAA, than D/L values. However, as would be expected, %FAA Asx increases over time at all

experimental temperatures (Fig. 8), and in the 'naturally aged' coral. A clear relationship is also apparent between %FAA Asx and THAA Asx D/L for both the high-temperature samples and 'naturally aged' samples (Fig. 9).
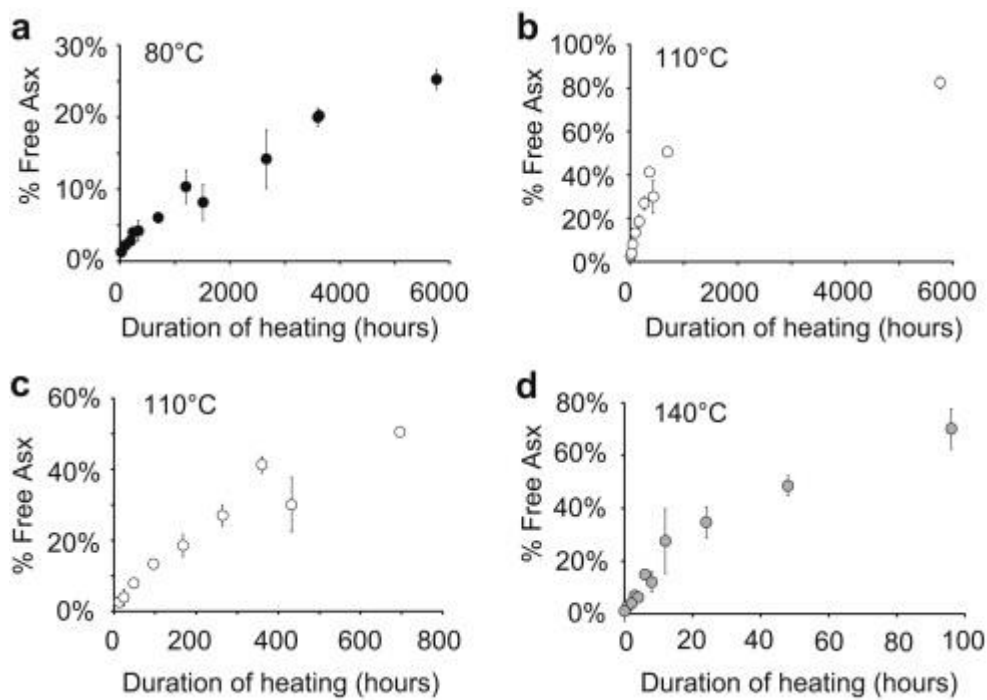
Fig. 8.
Percentage of free Asx vs duration of heating in hours, for samples heated at (a) 80 °C, (b) 110 °C, (c) 110 °C with shortened *x*-axis and (d) 140 °C. Each data-point represents the mean of the samples heated for the same duration at the specified temperature. Error bars represent ± 2 S.E. about the mean value. The sample heated at 110 °C for 432 h appears to deviate significantly from the expected trend. It is probable that this anomaly represents a compromised sample, though the cause of this is not clear (D/L values for this sample appear 'normal').
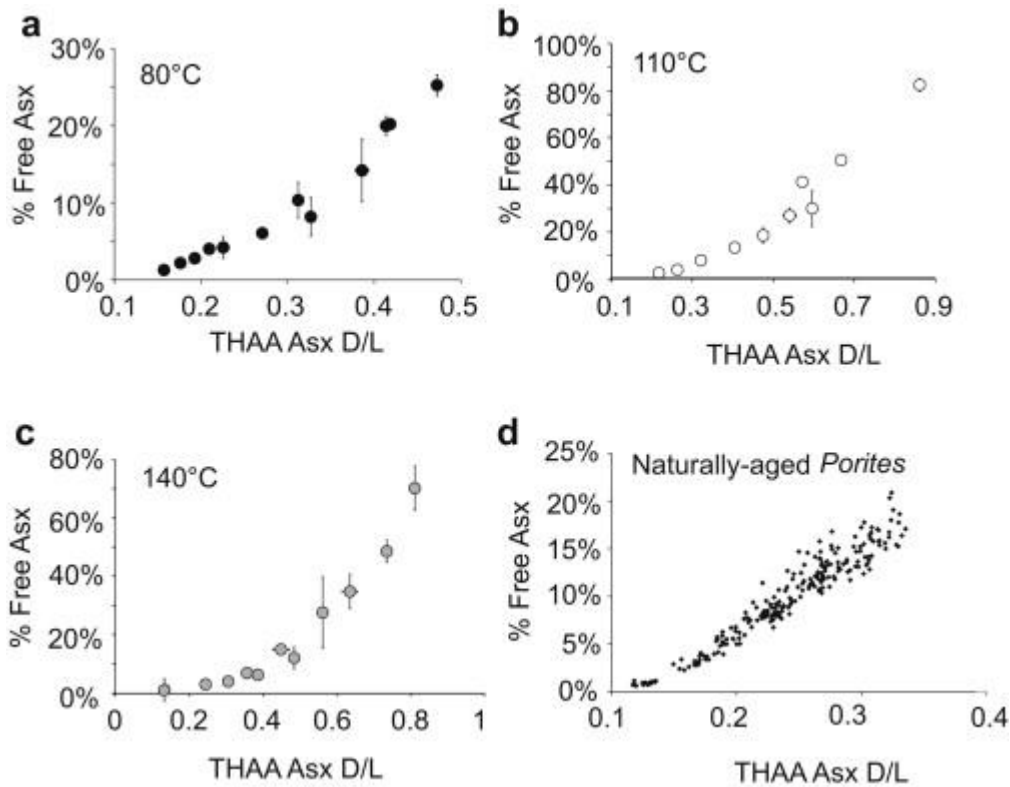
Fig. 9.
Percentage of free Asx vs Asx D/L for samples heated at (a) 80 °C, (b) 110 °C and (c) 140 °C and (d) 'naturally aged' samples. Each data-point represents the mean of the samples heated for the same duration at the specified temperature. For the 'naturally aged' coral, each data-point represents the mean of 2 analytical replicates. Error bars represent ± 2 S.E about the mean value.

3.5. Serine–alanine decomposition in *Porites* coral

The hydroxyl amino acid serine (Ser) is relatively unstable, and as protein degradation proceeds, Ser readily decomposes (by dehydration) into an end product of alanine (Ala) (Vallentyne, 1964 ; Bada et al., 1978). In the heated *Porites* coral, [Ser]/[Ala] displays a negative correlation with THAA Asx DL (Fig. 10a–c), and a similar trajectory is observed in the 'naturally aged' *Porites*, although variability about this trend is considerable (Fig. 10d).
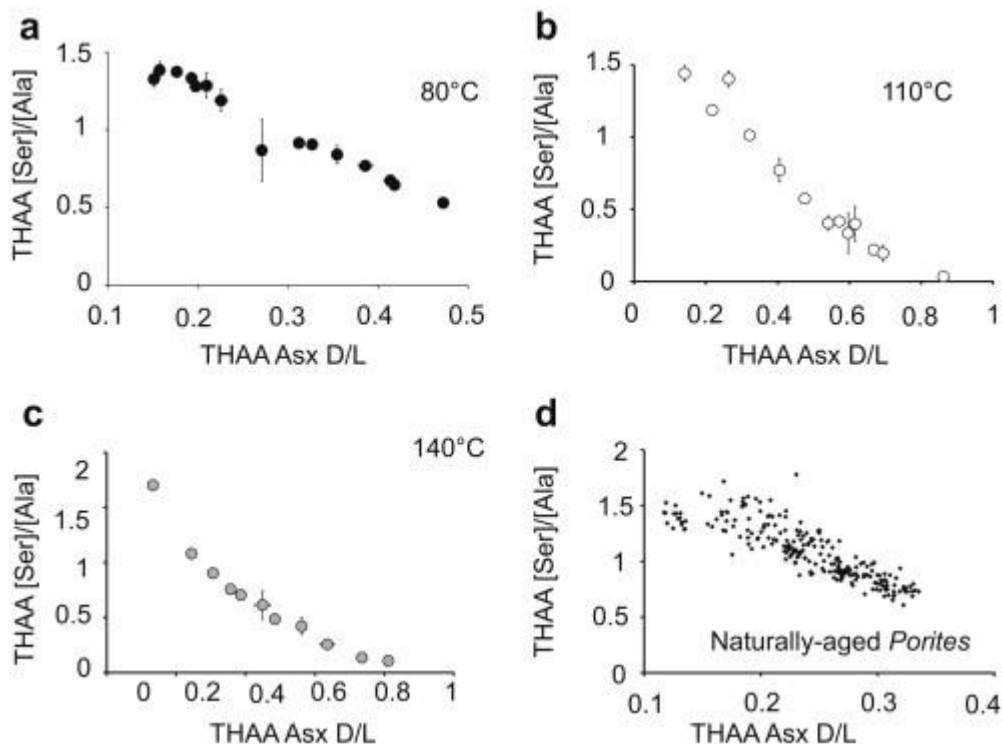
Fig. 10.
Graphs (a)–(d) show decomposition of serine to alanine ([Ser]/[Ala]) in the THAA fraction, normalised against THAA Asx D/L, for 80 °C, 110 °C, 140 °C and 26 °C respectively. For graphs (a)–(c), each data-point represents the mean of the samples heated for the same duration at the specified temperature. Error bars ± 2 S.E. about the mean. For the 'naturally aged' coral (d) each data-point represents the mean of 2 analytical replicates.

The decrease in [Ser]/[Ala] with time in 140 °C-heated *Porites* coral is shown in Fig. 11. Also plotted for comparison, are data derived from the marine gastropod mollusc *Patella* (Demarchi, 2009) and the opercula of the freshwater gastropod mollusc *Bithynia* (Penkman et al., 2008b), that have also been heated at 140 °C. The *Bithynia* opercula has the lowest initial [Ser]/[Ala] ratio, and demonstrates a lower rate of serine decomposition. Variability in the rates of decomposition exhibited by different species may be related to ease of free Ser generation; for example, given that peptide bonds involving aspartic acid are weak (e.g. Schultz et al., 1962; Qian et al., 1995 ; Goodfriend et al., 1992), the relatively high aspartic acid concentration in *Porites* coral (∼48%; Section 3.1) and *Patella* (∼32%; Demarchi, 2009), compared to *Bithynia* opercula (∼18%; Penkman et al., 2008a), may explain the faster release of Ser in the Asx-rich biominerals.
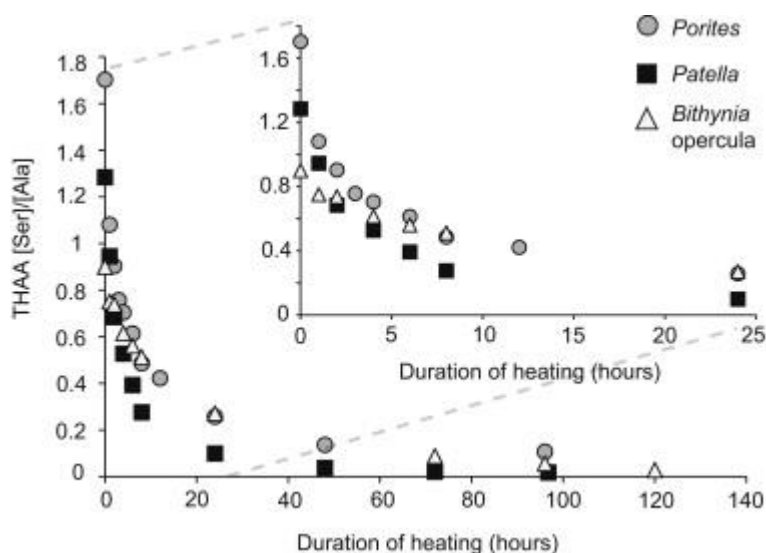
Fig. 11.
([Ser]/[Ala]) vs duration of heating at 140 °C for *Porites* coral (grey circles), *Patella* shell (black squares,Demarchi, 2009), and *Bithynia* opercula (white triangles, Penkman et al., 2008b). The inset graph expands the *x*-axis between 0 and 25 h.

The degradation of Ser into Ala (represented by [Ser]/[Ala]) may potentially be applied for geochronological purposes (as suggested by Bada et al., 1978; Bada and Man, 1980 ; Penkman et al., 2010). Westaway (2009) used a first-order rate equation to derive a rate constant for serine decomposition in *Bithynia* opercula that had been heated at 140 °C (Fig. 11) and, by extrapolating this rate down to an assumed temperature history, acquired numerical ages for fossil opercula. However, as is the case for *Patella* (Demarchi, 2009 ; Demarchi et al., 2013a), serine decomposition in *Porites* does not appear to follow an exponential relationship, which indicates that the calibration is not suitable for extrapolation. Indeed the presence of a residual bound fraction in biomineral observed in high-temperature studies on avian eggshell (Miller et al., 2000), terrestrial gastropods (Penkman et al., 2008a), and marine gastropods (Demarchi et al., 2013a), suggests that liberation of free Ser, and hence [Ser]/[Ala] decomposition, is unlikely to conform to a simple pseudo-first order relationship.

3.6. Comparisons of protein degradation in 'naturally aged' and experimentally heated *Porites* coral

Degradation patterns at elevated (80 °C, 110 °C, 140 °C) and ambient (26 °C) temperatures were compared to examine whether or not high-temperature experiments faithfully mimic degradation occurring in *Porites* coral *in vivo*.

While covariance between racemization of Asx and Glx in the THAA fraction appears to occur consistently at all temperatures (Fig. 12a), the relationship between the extent of Asx racemization in the THAA relative to the FAA fraction (Fig. 12b) is clearly temperature dependent; at lower temperatures the observed degree of racemization in the FAA fraction increases relative to the THAA fraction. Demarchi et al. (2013a) report a similar pattern in heated *Patella*; as was the case for corals, for a given THAA D/L value, FAA Asx D/L was generally higher at 80 °C, than at 110 °C and 140 °C.
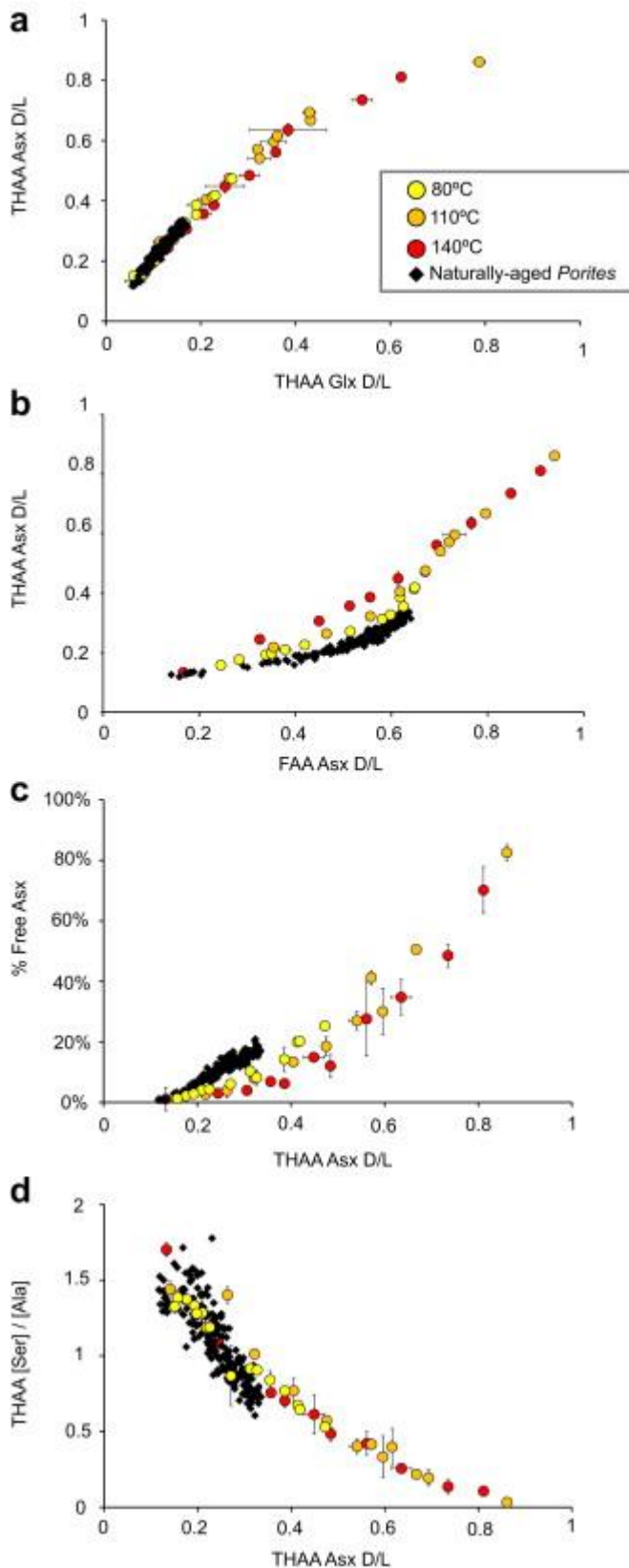
Fig. 12.
Graphs showing comparisons between protein degradation patterns at different temperatures; (a) covariance between racemization of Asx and Glx in the THAA fraction, (b) covariance between Asx racemization in the THAA and FAA fraction, (c) the relationship between %FAA Asx and the extent of Asx racemization in the THAA fraction, and (d) the relationship between the decomposition of Ser (represented by [Ser]/[Ala]) in the THAA fraction and the extent of Asx racemization. In all graphs, Red circles = samples heated at 140 °C, orange circles = samples heated at 110 °C, yellow circles = samples heated at 80 °C, black

diamonds = 'naturally aged' samples. All of the heat-treated samples were bleached prior to heating. For the experimental data (heat-treated samples), each data-point represents the mean of the samples heated for the same duration at the specified temperature. Error bars represent ± 2 S.E. about the mean. For the 'naturally aged' coral, each data-point represents the mean of 2 analytical replicates.

The relationship between the extent of hydrolysis (the %FAA) and the degree of racemization also varies between temperatures (Fig. 12c). At lower temperatures the generation of free Asx is higher, relative to a given THAA Asx D/L value. This disparity is very marked even between the 'naturally aged' samples and the lowest experimental temperature (80 °C). This pattern may suggest that increasing temperature induces a smaller change in the rate of hydrolysis than in the observed rate of racemization (i.e. that hydrolysis is less sensitive to temperature than racemization). Potentially, a reduction in the %FAA Asx relative to THAA D/L could also be a result of a greater loss (leaching) of free aspartic acid at higher temperatures. However, the low concentrations of FAA in the supernatant water, and the fact that the concentration of FAA in the supernatant water did not increase with temperature, indicate that leaching is not the cause of the observed patterns in intra-crystalline *Porites*. These patterns do not appear to be confined to Asx (see Fig. A8 of supplementary material), nor to *Porites* coral, as it has also been observed following heating experiments performed on *Patella*; as the temperature to which shells were heated decreased from 140 °C to 80 °C, the %FAA Asx increased for the same degree of THAA racemization (Demarchi et al., 2013a).

The relationship between [Ser]/[Ala] and THAA Asx D/L appears to follow a very similar trend at all three high-temperatures (Fig. 12d). This consistency between different high temperatures was also apparent in heated *Patella* (Demarchi, 2009). Comparisons with the 'naturally aged' samples are difficult due to the variability inherent in the data, and the limited range of values observed (compared to the heated samples).

The patterns observed here provide evidence that artificially induced protein degradation does not consistently replicate degradation at ambient temperatures in all amino acids in intra-crystalline *Porites*. This suggests that deriving reaction kinetics from high-temperature simulations for the amino acids discussed here is not necessarily valid. Similar patterns are also observed in heated *Patella* shell (Demarchi et al., 2013a) revealing that this observation is not limited to coral but also applies to other biominerals. However, the results suggest that heating at lower temperatures (though more time consuming) will better replicate degradation patterns observed in fossil samples. This is examined and discussed further in Section 3.7.

3.7. Arrhenius parameters for degradation reactions

In this study, we have measured racemization values (for both the THAA and FAA fractions) in 'naturally aged' material which (a) has been independently and accurately dated, (b) has a very well constrained temperature history, and (c) provides a large sample population size (>250 individual samples). In doing so, we are able to tightly constrain (and thereby improve) estimates of degradation reaction kinetics acquired from high-temperature data. This also provides a unique opportunity to investigate the models that are used to derive estimates of the rate and temperature sensitivity of degradation reactions. Here we discuss the application of two of the commonly used models, and present a new 'model-free' approach. We "quantitatively" compare the different techniques using the following method:

(i)

A value for the rate constant (k) for racemization was determined for each of the high temperature (80 °C, 110 °C, and 140 °C) experiments. Applying the Arrhenius relationship, these three rate constants were used to calculate an activation energy for racemization,

denoted (E_a). This E_a value acquired from the high-temperature experiments was subsequently used to "predict" a value for k at 26 °C (see Box 1), which is denoted here 'k^{exp26}'.

(ii)

A fourth rate constant for racemization was calculated using just the 'naturally aged' *Porites* coral samples; this is denoted here as 'k^{26}'.

(iii)

The difference between the values of 'k^{exp26}' and 'k^{26}' was determined; the degree of difference provides a means of assessing the limitations of the different methods used to estimate reaction kinetics.

Clearly, the ability to accurately predict the observed rate constant for the low temperature data (k^{26}) will also be related to the amount of variability within the 'naturally aged' coral samples, though this variability will be equal for all models when examining the same amino acid. For all calculations, a temperature of 26.2 °C (the average temperature at which GBR colonies grew; Hendy et al., 2012) was assigned to all the 'naturally aged' samples. Although the concentration of ~10 amino acids are determined by RP-HPLC, some of these amino acids are very minor components of the OM in *Porites* (Fig. 3), or can co-elute with other amino acids and are therefore not well resolved. The D/L (and %FAA) values for these amino acids are inherently associated with greater variability, and therefore deriving kinetic parameters from them is difficult and associated with greater uncertainty. Some models were "influenced" by this variability to a greater extent than others. Asx and Glx consistently provide the least "noisy" data due to their high concentrations in *Porites* OM, and so were examined in each of the models; where possible racemization (and hydrolysis) in other amino acids was also modelled. The low concentration of the FAA compared to the THAA fraction also means that FAA data is more variable, although due to its relatively high concentration in the OM, FAA Asx (and to some extent Glx) can provide adequate data.

3.7.1. Conventional approaches: reversible first order kinetic (RFOK) model

It has been demonstrated that reversible first order kinetics (RFOK) accurately describes free amino acid racemization in buffered aqueous solution (Bada, 1984 and references therein). If racemization kinetics follows RFOK then:
equation(5)

$$\text{L} - \text{amino acid} \underset{k_2}{\overset{k_1}{\leftrightarrow}} \text{D} - \text{amino acid}$$
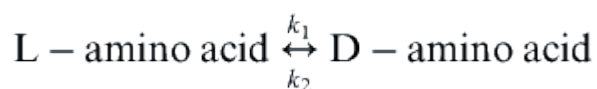
k_1 = forward rate constant; k_2 = reverse rate constant.
The rate expression for equation (5) is:
equation(6)

$$\frac{-\delta[\text{L}]}{\delta t} = k_1[\text{L}] - k_2[\text{D}]$$

t = time; [L] = concentration of L-enantiomers; [D] = concentration of D-enantiomers.
If k_1 is equal to k_2, then integrating and simplifying equation (6) gives:
equation(7)

$$\ln\left(\frac{1+[D]/[L]}{1-[D]/[L]}\right) = 2kt + \text{constant}$$

[D]/[L] = the amino acid enantiomeric ratio; constant = the small amount of D-enantiomer initially present in modern samples and formed by racemisation induced during sample preparation. Therefore, if AAR follows RFOK, then the "integrated rate equation" (Equation (7)), can be used to describe the relationship between the extent of racemization and time. In such a case, applying the integrated rate equation should linearise D/L values with respect to time (e.g. Bada and Schroeder, 1972), with a slope equal to 2k.

However, Asx racemization in bivalves (e.g. Manley et al., 2000) and gastropods (Goodfriend, 1991; Goodfriend and Meyer, 1991; Penkman et al., 2008a ; Demarchi et al., 2013a) does not conform to RFOK over the entire range of D/L values. Deviation from RFOK prior to equilibrium has also been observed in other amino acids (see Clarke and Murray-Wallace, 2006 and references therein). Therefore, the more "predictable" racemization kinetics of free amino acids in aqueous solution does not necessarily extrapolate to AAR occurring in proteins trapped within biominerals. Having established that racemization does not conform to first order reversible kinetics over the entire range of D/L values, several studies have instead applied the integrated rate equation over a specified interval; the "non-linear" approach (Wehmiller and Belknap, 1978). This interval typically represents the initial phase of the racemization reaction up to a specified D/L value (Clarke and Murray-Wallace, 2006 and references therein). It is the more slowly racemizing (epimerizing) amino acids, particularly isoleucine, that appear to adhere most strongly to RFOK and can be linearised to higher D/L values than rapidly racemizing amino acids, such as aspartic acid (e.g. Goodfriend, 1991; Brooks et al., 1990 ; Miller et al., 2000). Alternatively, the integrated rate equation has been applied sequentially over two or more separate linear phases, deriving individual k values for each (see discussions in Wehmiller and Hare, 1971; Bada and Schroeder, 1972; Schroeder and Bada, 1976; Kriausakul and Mitterer, 1978 ; Wehmiller and Belknap, 1978). When ln[(1 + D/L)/(1 − D/L)] Asx and Glx values observed in this study of *Porites* are plotted against time, the data is characterised by an initial rapid and a secondary slower phase, and therefore deviates considerably from a linear relationship; this is true for both the THAA and FAA fractions (Fig. A9 of the supplementary material) and for THAA Ala, phenylalanine (Phe) and valine (Val), which are also found in reasonably high concentrations in the OM of *Porites* coral (Fig. 3). Indeed if sufficiently high densities of data were available across the full extent of the reaction, many more 'phases' could potentially be identified, in what is a continually changing process.

The lack of conformity to RFOK in skeletal proteins is unsurprising. Even in a closed-system (i.e. where products of degradation are retained and contamination excluded) the extent of racemization observed is, in reality, the product of a complex network of parallel reactions (Kriausakul and Mitterer, 1978; Wehmiller, 1993 ; Penkman et al., 2008a). Aspartic acid appears to follow particularly unusual kinetic patterns when compared to other amino acids, with especially "rapid" and "slow" components observed (see Collins et al., 1999). Asx D/L is actually the combined signal of aspartic acid (Asp) and asparagine (Asn) and, atypically for amino acids, both can racemize as bound residues via the formation of a cyclic succinimide intermediate (Geiger and Clarke, 1987), facilitating rapid racemization rates during the early stages of diagenesis. However, the rate of succinimide formation is an order of magnitude faster in Asn (Geiger and Clarke, 1987) and it has been suggested (Goodfriend, 1991) that this difference may contribute to the "atypical" pattern of Asx racemization. Furthermore, the ease of succinimide formation is likely to increase with time as higher order structures of the proteins, which restrict succinimide formation, breakdown (see Waite and Collins, 2000). This initial burst of racemization

then slows dramatically, probably as Asx residues are hydrolysed to terminal and free positions. Conversely dense sampling of the early phase of racemization in hydrophobic amino acids such as Ile reveals a marked initial lag phase (Demarchi et al., 2013a), prior to the generation of the first residues in N-terminal positions able to undergo epimerization (Mitterer and Kriausakul, 1984). Since racemization in Asx, Glx, Ala, Phe and Val in *Porites* coral does not conform to RFOK over the entire extent of the reaction, values for k were calculated over two different intervals; a rapid interval (k^{fast}) and a second slower interval (k^{slow}). The break-in slope (delimiting the two intervals) was initially chosen visually, but was "fine-tuned" by partitioning data-points in close proximity to the chosen break-in-slope between the fast and slow phases, to gain the highest possible combination of r^2 values. This was performed for Asx, Glx, Ala, and Phe (though not for Val due to the high degree of variability in the 'naturally aged' *Porites*) for the THAA fraction, and Asx and Glx for the FAA fraction, as these amino acids exhibited D/L values that were sufficiently well constrained to enable meaningful determination of k. Values for k^{fast} and k^{slow} are given in Table A3 of the supplementary material (and plots for THAA and FAA Asx are shown in Fig. A9 of the supplementary material). In this study, regression lines were not forced through the initial D/L value; in all biominerals, even if a constant is subtracted from observed D/L values, this initial data-point will not truly represent the origin of the reaction, and given that the aim is to derive a value for k, there appears to be no reason to bias this initial data-point by fixing the regression line through it. At each temperature, the k^{fast} for THAA racemization (in Asx, Glx, Ala and Phe) was generally between ~3 and 6 times faster than k^{slow}, while for the FAA, the difference was higher (often approaching or greater than an order of magnitude difference). Similarly, Wehmiller and Belknap (1978) reported differences of almost an order of magnitude between k values derived from fast and slow linear components for epimerisation of isoleucine in molluscs.

Applying the integrated rate equation over a select interval naturally means that the value of k derived will not be representative of the entire reaction. Furthermore, if the k values calculated at each temperature from the specified (i.e. initial) interval are to be used to estimate the temperature dependence (E_a) of the observed reaction, then the estimates of E_a are again only applicable over the specified interval (Wehmiller and Belknap, 1978). In addition, this approach is sensitive to the choice of the linear interval limit (or break in slope if two linear components are modelled). The break in linearity is often poorly defined (e.g. Fig. A9 of the supplementary material) and inclusion or exclusion of data-points in close proximity to the limit can cause relatively large changes in the slope of the line, and therefore the value of k. If values for k are to be calculated over two different intervals, the choice of break in slope between the successive linear phases is also influenced by the range and density of D/L values measured. It is clear from the 110 °C experimental data, that when the highest time point (5760 hours) is included, it becomes necessary to fit a third linear component (Fig. A9b of the supplementary material). Lastly, the regression line for the initial linear segment may (e.g. Bada, 1972) or may not (e.g. Goodfriend and Meyer, 1991) be forced through the first time point, which will influence the slope (and therefore k) of the regression line.

In addition to the well-established issues discussed above, we found that the accuracy of the k values derived at 26 °C was compromised by the scatter in the 'naturally aged' coral data-set (as represented by the lower r^2 values in Fig. A9d and h of the supplementary material). Also, the apparently high r^2 values determined for the regression line in Arrhenius plots can sometimes be misleading, and are often an artefact of the low (effective burial) temperature k value. For example, in the Glx Arrhenius plots (Fig. A10c and d of the supplementary material), the k values show a noticeable degree of scatter about the linear regression line despite high (>0.96) r^2 values. This is obviously not just a limitation of the RFOK model, but should be considered in all cases in which temperature sensitivity is estimated using Arrhenius plots.

Despite the limitations discussed, the E_a derived from just the high-temperature k values, predicts the value of k at 26 °C (k^{exp26}) reasonably well for THAA Asx (only 1.15 and 1.13 times slower than the 'observed' rate constant for the 'naturally aged' coral, for the fast and slow interval respectively). This was not the case however for some other amino acids (Fig. 13 and Table 2). As would be expected, where D/L values were associated with less variability (e.g. THAA Asx and THAA Glx) the model performed better than where variability was greater (e.g. THAA Ala, THAA Phe, FAA Glx). In all cases, when the 'naturally aged' k value was omitted and only the experimental k values applied, the E_a changed, in some cases quite considerably (Table 2), demonstrating the significance of constraining high-temperature rates with those acquired at lower (e.g. burial) temperatures (e.g. Kaufman, 2006).
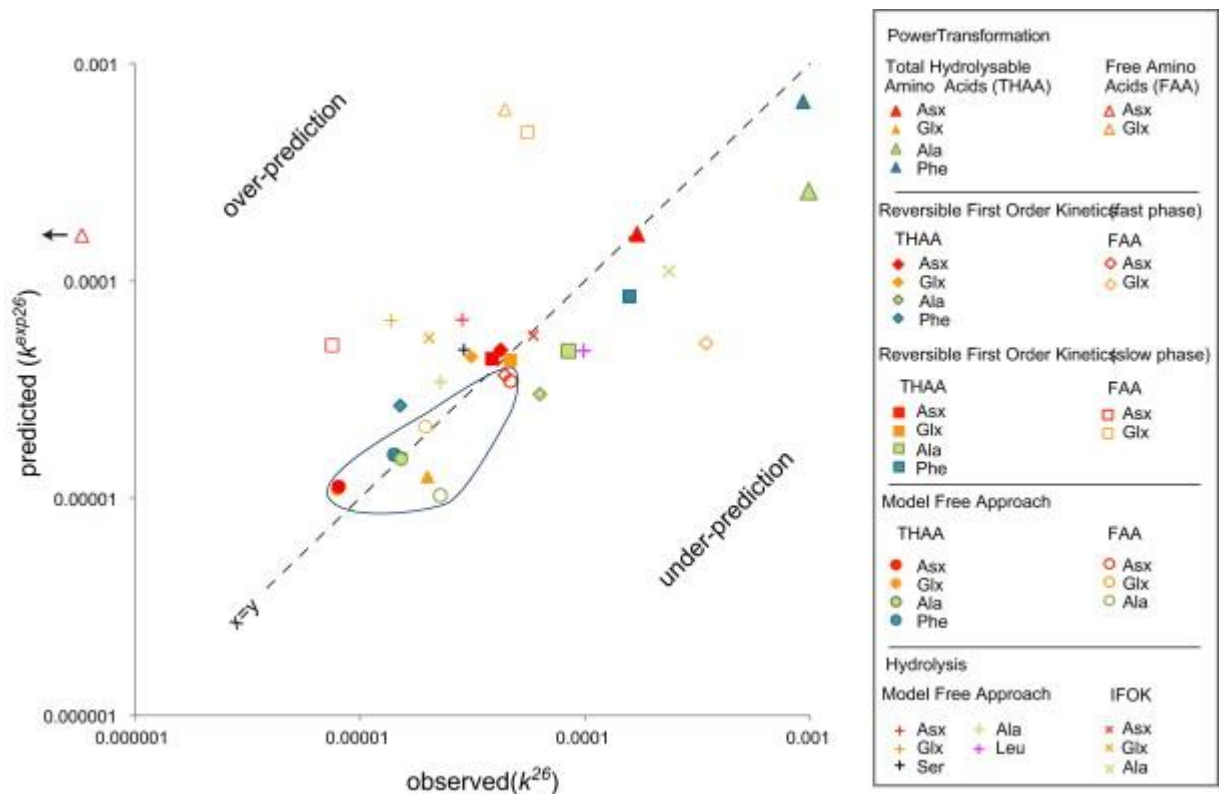
Fig. 13.
Plot of predicted (k^{exp26}) vs observed (k^{26}) rates. Rates for racemization have been derived using an 'RFOK' model (initial linear component = diamonds, secondary linear component = squares), 'power-function' model (triangles), and a 'model-free' approach (circles) and are reported relative to the rate at 110 °C. Open symbols represent FAA values, while closed symbols represent values obtained from the THAA fraction. Values acquired using the 'model-free' approach have been encircled. In addition to racemization, rates were also calculated for hydrolysis using the 'model-free' approach (+ symbol) and using an irreversible first order kinetic (IFOK) transformation (× symbol). The data has been plotted on a log vs log scale. The closer the predicted (k^{exp26}) value is to the observed value at 26 °C (k^{26}), the closer the point will lie to the $x = y$ line. Note the power model value for FAA Asx racemization lies outside the plotted area.

Table 2.
Activation energies (E_a) calculated for racemization using the RFOK model (both the initial fast, and secondary slow intervals), power-function model, and 'model-free' approach. For the RFOK and power-function model, the D/L range over which k was calculated is provided for each temperature. For the 'model-free' approach, the range of D/L values over which differences between the polynomial fits were calculated (see main text for details) is given. E_a values have been calculated with and without the naturally aged (26 °C) *Porites* coral data. The E_a derived using k values from just the experimental data (80 °C, 110 °C, 140 °C) has been used to

'predict' a value for k at 26 °C (k^{exp26}; see text for details), which is compared to the 'actual' rate constant (k^{26}) calculated from the 'naturally aged' coral.

	Fitting range (D/L)				E_a 26–140 °C (kJ mol⁻¹)	E_a 80–140 °C (kJ mol⁻¹)	Comparison of k^{exp26} relative to k^{26}
	26 °C	80 °C	110 °C	140 °C			
RFOK (fast) model							
THAA Asx	0.12–0.25	0.14–0.28	0.14–0.41	0.14–0.48	115	117	1.15 times slower
THAA Glx	0.06–0.12	0.06–0.15	0.06–0.22	0.06–0.23	119	122	1.44 times slower
THAA Ala	0.07–0.33	0.09–0.30	0.09–0.51	0.09–0.52	121	114	2.04 times faster
THAA Phe	0.06–0.23	0.03–0.17	0.03–0.31	0.03–0.33	126	131	1.76 times slower
FAA Asx	0.12–0.22	0.15–0.28	0.14–0.41	0.13–0.48	115	114	1.20 times faster
FAA Glx	0.17–0.56	0.2–0.38	0.33–0.50	0.2–0.31	116	98	6.67 times faster
RFOK (slow) model							
THAA Asx	0.20–0.34	0.31–0.47	0.47–0.69	0.56–0.82	116	118	1.13 times slower
THAA Glx	0.09–0.17	0.16–0.27	0.26–0.44	0.23–0.62	118	117	1.08 times faster
THAA Ala	0.29–0.41	0.56–0.76	0.55–0.83	0.29–0.41	113	108	1.77 times faster
THAA Phe	0.13–0.28	0.14–0.39	0.35–0.60	0.08–0.68	111	105	1.86 times faster
FAA Asx	0.53–0.64	0.59–0.67	0.62–0.80	0.61–0.91	118	136	6.71 times slower
FAA Glx	0.24–0.71	0.34–0.47	0.49–0.55	0.23–0.68	105	125	8.75 times slower
Power-function model							
THAA Asx	0.12–0.34	0.14–0.47	0.14–0.86	0.14–0.82	110	110	1.04 times faster
THAA Glx	0.06–0.17	0.06–0.27	0.06–0.80	0.06–0.62	129	125	1.59 times faster
THAA Ala	0.07–0.41	0.09–0.53	0.09–0.96	0.09–0.83	100	87	3.81 times faster
THAA Phe	0.06–0.28	0.03–0.39	0.03–0.85	0.03–0.68	92	89	1.39 times faster
FAA Asx	0.14–0.64	0.17–0.67	0.17–0.94	0.17–0.91	112	175	772.45 times slower
FAA Glx	0.17–0.71	0.20–0.47	0.33–0.86	0.33–0.68	93	118	14.01 times slower
Model-free (scaling) approach							
THAA Asx	0.19–0.71				131	134	1.46 times slower

	Fitting range (D/L)				E_a 26–140 °C (kJ mol^{-1})	E_a 80–140 °C (kJ mol^{-1})	Comparison of k^{exp26}relative to k^{26}
	26 °C	80 °C	110 °C	140 °C			
THAA Glx	0.08–0.70				132	135	1.44 times slower
THAA Ala	0.14–0.83				127	127	1.03 times slower
THAA Phe	0.08–0.59				125	126	1.15 times slower
FAA Asx	0.35–0.79				117	114	1.3 times faster
FAA Glx	0.3–0.55				118	119	1.13 times slower
FAA Ala	0.50–0.85				130	124	2.14 times faster

Table options

3.7.2. Conventional approaches: irreversible first order kinetic (IFOK) model for hydrolysis

The rate of hydrolysis was examined by applying irreversible first order kinetics (equation (8)), as was done previously by Miller et al. (1992) to estimate Leu hydrolysis rates.

$$\text{Observed rate of hydrolysis} = \left(\frac{-\delta[\text{Bound}]}{\delta t} \right) = [\text{Bound}]k$$

equation(8)

[Bound] = the concentration of peptide-bound amino acids, calculated using (THAA concentration − FAA concentration); k = observed rate constant for hydrolysis; t = time. Equation (8) equates to the integrated rate law:
equation(9)

$$\ln\left[\frac{[\text{Bound}]}{[\text{Total}]} \right] = -kt$$

[Total] = the total concentration of amino acids present.
As hydrolysis proceeds, the peptide chain will become more fragmented, resulting in a lower proportion of bound amino acids, and so we would expect the [bound]/[total] value (and the ln[bound]/[total] value) to decrease with time. However, due to greater variability in the data, a greater degree of error will be inherent in estimates of amino acid hydrolysis when compared to estimates for racemization. Three amino acids, Asx, Glx, and Ala, provided adequate data to enable estimates of hydrolysis rates (though Leu and Ser showed an obvious negative relationship with time, there was too much variability to adequately linearise the data, particularly for the 'naturally aged' samples). The total amino acid concentration expressed in equation (9) was calculated individually at each time point, to partially compensate for decomposition of amino acids. If hydrolysis conforms to irreversible first order kinetics (IFOK), then plotting ln([THAA] − [FAA])/[THAA] against time should yield a straight line, with a gradient equal to the observed rate constant (−k) for hydrolysis.
The relative extent of free amino acid liberation was Ala > Asx > Glx (e.g. heating for 3600h at 80 °C, provided [bound]/[total] values of ~0.37. ~0.80, and 0.90, for Ala, Asx, and Glx, respectively). This same relative ordering was also observed by Demarchi et al. (2013a) in *Patella*.

The decomposition of free Ser into free Ala (Vallentyne, 1964 ; Bada et al., 1978), is likely to account, at least to some extent, for the apparent rapid decrease in the [bound]/[total] values for Ala; although in our calculations we attempt to account for decomposition of amino acids into simpler molecules, it is much more difficult to account for decomposition of one amino acid into another. On the other hand, the relatively high [bound]/[total] Glx values are (at least in part) likely to be a consequence of reversible lactamisation of free Glx forming pyroglutamic acid, thereby causing an underestimation of FAA Glx, and so an overestimation of Glx in the bound state. That said, given its slow rate of racemization (for which hydrolysis is required), it is likely that Glx hydrolysis is indeed, relatively slow in comparison to other amino acids. Such considerations highlight the potential difficulties in accurately estimating true degradation reaction rates in such a complex system.

Ala and Asx hydrolysis appears to follow IFOK to similar [bound]/[total] values (~0.2 and ~0.25 respectively), while Glx deviated significantly from IFOK much more rapidly, after [bound]/[total] values of ~0.9. At [bound]/[total] values lower than these limits, values decreased more slowly in all amino acids than would be predicted by IFOK (reflecting a slowing in the rate of hydrolysis). Miller et al. (1992) also noted a decrease in the rate of hydrolysis of Leu following an initial linear period, and attributed this to variable bonding strength between Leu and other amino acids in the polypeptide chain, modulated by decomposition reactions.

Here, observed k values for Asx, Glx, and Ala hydrolysis were derived from only the initial linear (IFOK) phase, using the [bound]/[total] cut-off value of 0.25, 0.914 and 0.2, respectively (see Fig. A11(a)–(h) of the supplementary material for plots of Asx and Glx). Once applied in an Arrhenius plot, these yielded E_a values of 111, 115 and 106 kJ mol^{-1}for Asx, Glx and Ala respectively (Table 3). For each amino acid, the E_a calculated for hydrolysis using IFOK is below the E_a calculated using RFOK (applying k from either the Fast or Slow linear segment) for racemization (Fig. 14c).

Table 3.

Activation energies (E_a) calculated for hydrolysis using the IFOK and 'model-free' approach. For the IFOK model, the values of k used to derive the E_a estimates were determined from just the initial range of [bound]/[total] values that conformed to linear irreversible first order kinetics (see Section 3.7.2 of main text for details). The 'model-free' approach was used to derive E_a values for hydrolysis for five amino acids (Asx, Glx, Ala, Ser, and Leu), but only the first 3 AAs provided adequate data to enable estimates of hydrolysis rates using the IFOK model. For the IFOK model estimates, the %FAA equivalent for the range of [bound]/[total] values used to derive values for k at each temperature (i.e. the range over which data conformed to IFOK) is shown. For the 'model-free' approach, the range of %FAA values over which differences between the polynomial fits were calculated (see main text for details) is given. E_a values have been calculated with and without the naturally aged (26 °C) *Porites* coral data. The E_a derived using k values from just the experimental data (80 °C, 110 °C, 140 °C) has been used to 'predict' a value for k at 26 °C (k^{exp26}; see text for details), which is compared to the 'actual' rate constant (k^{26}) calculated from the 'naturally aged' coral.

	Fitting range (%FAA)				E_a 26–140 °C (kJ mol^{-1})	E_a 80–140 °C (kJ mol^{-1})	Comparison of k^{exp26}relative to k^{26}
	26 °C	80 °C	110 °C	140 °C			
IFOK							
Asx	<21%	<26%	<51%	<74%	111	111	1.04 times faster
Glx	<9%	<9%	<9%	<8%	115	125	2.77 times slower
Ala	<73%	<74%	<80%	<92%	106	99	2.1 times faster
Model-free (scaling) approach							
Asx	2–54%				112	120	2.44 times slower
Glx	1–12%				116	131	5.01 times slower
Ser	5–58%				116	121	1.73 times slower
Ala	10–79%				116	120	1.55 times slower

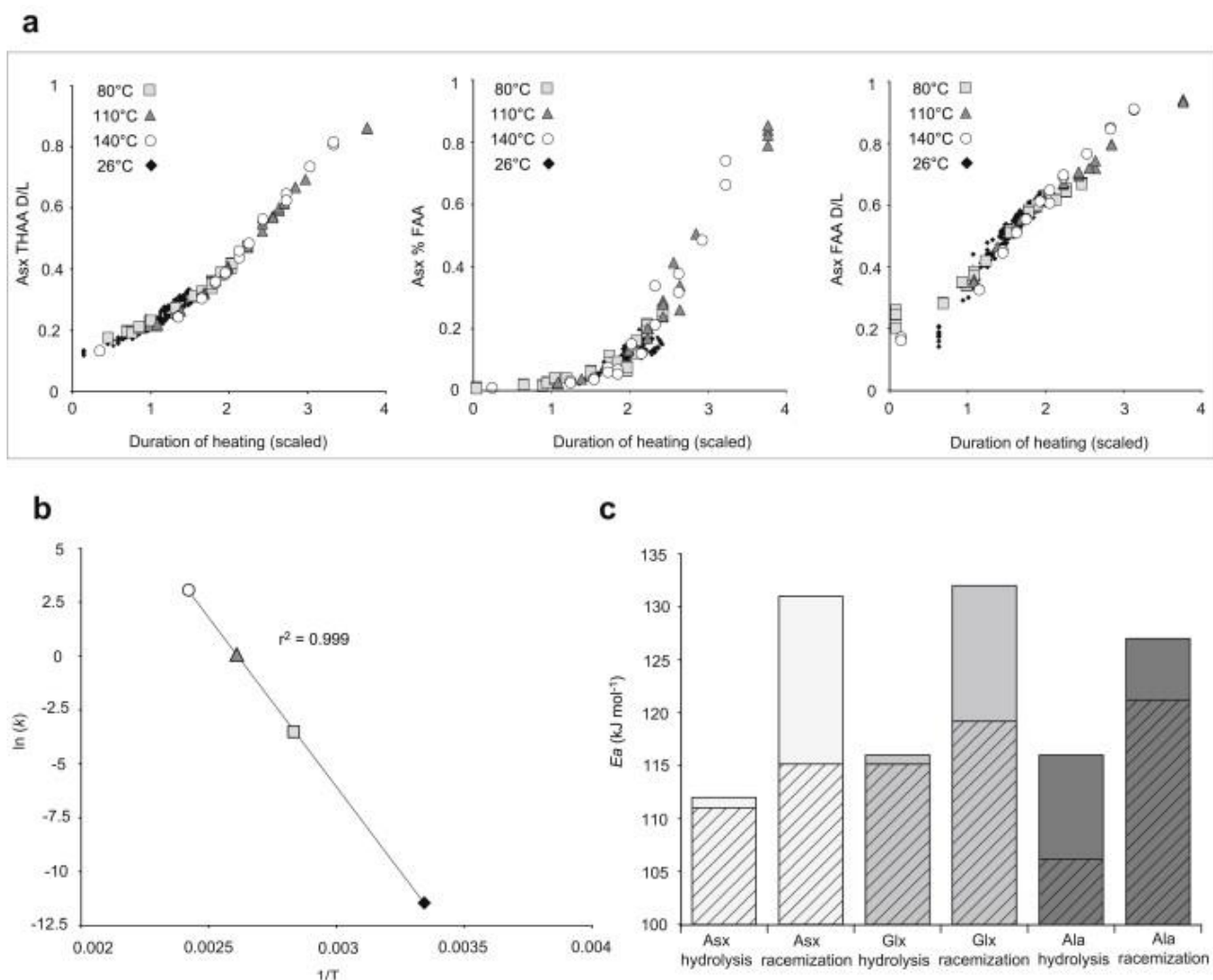|	Fitting range (%FAA)				E_a 26–140 °C (kJ mol^{-1})	E_a 80–140 °C (kJ mol^{-1})	Comparison of k_{exp26} relative to k_{26}
	26 °C	80 °C	110 °C	140 °C			
Leu	5–51%				112	105	2.01 times faster

Table options

Fig. 14.

(a) Overlay of THAA Asx D/L values, Asx %FAA values and FAA Asx D/L values collected at different temperatures, plotted using the 'model-free' approach. The abscissa (x-axis) has been scaled in each graph (see text for details of how scaling was applied). The degree to which the abscissa is scaled at each temperature, can be used to derive a value for k relative to 110 °C (k^{rel}). (b) Arrhenius plot for THAA Asx racemization with relative rate constants (k^{rel}) derived using the 'model-free' approach. White circle = k^{rel} for D/L values acquired at 140 °C, dark grey triangle = k^{rel} for D/L values acquired at 110 °C, grey square = k^{rel} for D/L values acquired at 80 °C, black diamond = k^{rel} for D/L values acquired at 26 °C,. (c) Comparison between (effective) activation energy values for THAA racemization and hydrolysis (for Asx, Glx and Ala), calculated using the entire temperature range of 26–140 °C. Patterned bars represents E_a values derived using irreversible first order kinetics (IFOK) for hydrolysis, and reversible first order kinetics (RFOK; initial fast stage) for racemization. Open bars represent effective activation energy (E_a) values derived using the 'model-free' approach. On all occasions the (effective) E_a for hydrolysis is lower than for racemization (irrespective of which technique is used to derive the observed rate constant).

Figure options

This technique suffers from some of the same issues encountered when applying RFOK to racemization data; for example, the value of k derived will not be representative of the entire reaction and will be sensitive to the subjective choice of the start and end points of the linear interval (again influenced by the range and density of values measured). However, for THAA Asx hydrolysis, the E_a derived from only the high-temperature (80 °C, 110 °C and 140 °C) rate constants appears to "predict" a value of k at 26 °C (k^{exp26}) that is very close to the value of k actually observed in the 'naturally aged' *Porites* (k^{26}) (Table 3 and Table A5 of the supplementary material), also demonstrated by the very high r^2 value for the regression line in the Asx Arrhenius plot (Fig. A11i of the supplementary material). In light of the complexity of underlying reactions contributing to our measure of hydrolysis, it is unlikely that the reaction, in reality, conforms to IFOK. Also, given the degree of variability in the 'naturally aged' data (Fig. A11d of the supplementary material), the accuracy of this prediction for Asx appears somewhat "fortunate". However, the results do suggest that high temperature data can be applied with this model to estimate, with reasonable accuracy, observed rates of hydrolysis at low temperatures for Asx up to [bound]/[total] values of 0.25. In contrast, this was not the case for Glx and Ala, for which k^{exp26} and k^{26} differed considerably (Table 3).

3.7.3. Conventional approaches: mathematical models (the power-function transformation)

An alternative approach is to use mathematical expressions to linearise the relationship between racemization and time, and then calculate rates directly from these. Several different empirically based transformations have been used (see Clarke and Murray-Wallace, 2006 for examples), though probably most common are power-function transformations (e.g. Goodfriend et al., 1995; Goodfriend et al., 1996; Kaufman, 2000; Kaufman, 2006 ; Manley et al., 2000). In this study, we attempted to linearise Asx, Glx, Phe and Ala THAA D/L, and Asx and Glx FAA D/L values by applying a simple power-law function (equation (10));
equation(10)

$$nD/L = kt + constant$$

n = the exponent that produces the best linear relationship between D/L and t.
As recommended by Kaufman (2000), the value of the exponent (n) was changed in increments of 0.1 to obtain a value that best linearised the data (as determined by the highest r^2 value) over the entire range of D/L values measured. Power-transformed D/L values were plotted against time (see Fig. A12 of the supplementary material for an example of THAA and FAA Asx) and values for k were calculated from the slope of the linear regression line (Table A3 of the supplementary material). As before, the E_a derived from just the high-temperature data (80 °C, 110 °C and 140 °C) was used to predict k^{exp26}, which can subsequently be compared with k^{26}, the "actual" rate constant calculated from just the 'naturally aged' specimens (Fig. 13, Table 2 and Table A4 of the supplementary material).
Due to the nature of the power-transformation, the linear regression line that is fitted to the power-transformed data generally overestimates the rate of increase at low D/L values, with higher D/L values imparting greater influence on the regression line than initial values (see Fig. A12 of the supplementary material for an example). This is true particularly at higher temperatures (e.g. Goodfriend et al., 1996 ; Manley et al., 2000; and this study) and contrasts with the RFOK model (which as described previously, is usually split to derive estimates of early and later phases of the reaction).

In almost all cases the k values calculated using the power-transformation were lower than those acquired from either the fast or slow linear components of the RFOK model (Table A3 of the supplementary material). The E_a values derived using the power-transformation approach differed quite considerably (Table 2), though not systematically, from the E_a values estimated using the RFOK model (e.g. Asx ~ 5–6 kJ mol^{-1} lower; Glx ~ 10 kJ mol^{-1} higher, using the power-transformation). As with the RFOK model, this approach predicted rates in the 'naturally aged' coral (k^{exp26}) with greater success for the THAA fraction than the FAA fraction (Fig. 13, Table 2). Given that the FAA Asx is reasonably well constrained (almost certainly more so than THAA Ala and Phe), this may not simply be a consequence of greater variability in the FAA data sets. For all the amino acids tested however (with the exception of Glx), the fit to a linear relationship in the Arrhenius plots was relatively weak (e.g. for Asx in both the THAA and FAA fractions, see Fig. A12i and k of the supplementary material).

Examining the temperature sensitivity of aspartic and glutamic acid in the foraminifera *Pulleniatina*, Kaufman (2006) linearised D/L values using simple power law kinetics, but truncated the time series at Asp D/L < 0.5, and Glu D/L < 0.25, as only over this range did the transformation provide satisfactory linearisation across all temperatures. Though infrequently applied, this method enables direct comparison of a specified "phase" of the racemization reaction at all the temperatures tested. Here, we re-applied the power transformation after truncating D/L values to 0.5 (Asx), 0.3 (Glx), 0.55 (Ala) and 0.45 (Phe). The D/L limits selected for each amino acid are subjective, but were chosen to best linearise the initial stages of racemization. For all four amino acids, D/L values only reached above these limits at 110 °C and 140 °C, and in these cases, a slightly different (always lower) value for the exponent (n) was required to best-linearise the data. It was noticeable from the 'D/L$_n$ vs time' plots, that in most cases the regression line better approximated the lower D/L values in the truncated data-set, than had previously been the case, when due to the "pull" of higher-D/L data points, lower data-points were commonly over-estimated by the regression line (e.g. compare Figs. A12b and c and A13a and b, of the supplementary material).

For all the amino acids tested, truncating the data sets at 110 °C and 140 °C resulted in an increase in the value of k for that temperature, as may be expected given the slowing of the rate of racemization at higher D/L values. Increasing the highest-temperature (110 °C and 140 °C) k values subsequently resulted in a steeper regression line in the Arrhenius plots, and therefore a rise in the E_a value for each amino acid relative to the values obtained using the full data set (see Fig. A13c and Table A4 of the supplementary material). This increase was considerable, particularly for THAA Asx and THAA Glx, which increased from 110 to 129 kJ mol^{-1}, and 129–141 kJ mol^{-1}, respectively. Also, while use of the full (non-truncated) data-set for the THAA fraction consistently predicted a k^{exp26} value higher than the k value observed in the 'naturally aged' coral (i.e. $k^{exp26} > k^{26}$), for THAA Asx, Glx and Phe, using the truncated data set resulted in predicted k values below the observed k value in the 'naturally aged' *Porites* (i.e. $k^{exp26} < k^{26}$; see Table A4 in the supplementary material). The exception to this was Ala, which maintained a $k^{exp26} > k^{26}$ when data was truncated. For all four amino acids, the predictions of k^{exp26} from the truncated data-set were consistently (and for Asx and Glx, considerably) further from the observed k value for the 'naturally aged' *Porites* (k^{26}) than when the power transformation was applied to the full-data set (see Table A4 of the supplementary material). In addition, we noted that relatively small variations in the subjectively chosen D/L-limit sometimes influenced the estimated E_a to a large extent. For example, for THAA Glx, varying the D/L limit between 0.25 and 0.35, provided E_a values ranging from about 121 to 138 kJ mol^{-1}, while for more poorly constrained amino acids (e.g. Phe), the choice had an even greater influence. As was the case with the RFOK model, the E_a estimated using a limited data-set will only apply to that phase of the entire

reaction. It was not possible to truncate and examine the D/L data for FAA Asx and Glx in the same way as the THAA data, due to the very low concentrations, and therefore higher variability observed in the initial phase of racemisation in this fraction.

It is clear therefore, that there are limitations to modelling racemisation kinetics either by using a simple kinetic model (Section 3.7.1), or by applying a mathematical transformation. RFOK model fitting tends to prejudice in favour of the early phase of racemization (hence often resulting in the decision to fit two alternative rates to the "fast" and "slow" components), whilst power transformations can prejudice the most highly degraded samples. Both sets of approaches can be compromised by the data captured; the greater the sampling density at particular time ranges, the more apparent it is that the initial rates of racemization are either extremely fast (e.g. Asx; see Goodfriend et al., 1995; Brinton and Bada, 1995 ; Wait and Collins, 2000) or atypically slow (e.g. Ile; Miller et al., 1992); in the former case because of succinimide mediated racemization of bound residues, in the latter case due to the need to cleave Ile residues to terminal positions. The longer an experiment is run, the more dominated the rate estimates become by the slow rate observed for a residual component, which appears to be a common feature of all long-term diagenesis experiments (e.g. Miller et al., 2000; Penkman et al., 2008a ; Demarchi et al., 2013a). The cause of this slowing in the rate of reaction is unclear; it may be a result of limits in water availability, or the presence of hydrophobic stretches resistant to hydrolysis (see discussion in Wehmiller, 1980 ; Collins and Riley, 2000). Whatever the reason, the net effect is that the longer the period over which data is collected, the slower the rate that is estimated when a power transformation is applied. In the case of RFOK, a longer period of data collection will affect both the choice of the break-point in slope and the rate of the second slow phase. The problem is exacerbated because at lower temperatures the time scales required to capture the range of reactions are impractical; for example to get an equivalent data set in *Porites* coral to that observed by Miller et al. (1992) for Ile racemization in ostrich eggshell (to reach an alle/Ile ratio of ~1.3 required about 1 month at 142.5 °C), would take an estimated ~50 years at 80 °C, assuming an E_a of 125 kJ mol^{-1}. There is therefore potential for a systematic error in the Arrhenius estimates generated using high temperature data, because only the highest temperature experiments fully encompass the slowing in racemization and hydrolysis rate.

3.7.4. A novel 'model-free' approach and implications for high-temperature simulation experiments

We propose an additional alternative approach to estimate Arrhenius parameters, which (like the power transformation) is not based on assumptions regarding the underlying kinetics of the system. Instead it attempts to maximise the correspondence between different temperature experiments, by scaling the time axis (abscissa) to maximise the overlap of all the data, thereby embracing the complex patterns often formed in amino acid racemization and decomposition kinetics.

To capture the initial pattern of degradation the time scale was log-transformed (this also reduces the emphasis on the final time point, which can be a limitation of power transformations). As a zero time point cannot be included on a log scale, we fixed the initial value (which represents both decomposition/racemization in the sample prior to analysis and that induced during sample preparation) at log − 1 (although this initial value was not included in the scaling algorithm for the abscissa).

The abscissa was then scaled between neighbouring temperatures (i.e. between 26 °C and 80 °C, between 80 °C and 110 °C, and between 110 °C and 140 °C) for the range over which the ordinate data for each temperature "pair" overlapped (the polynomial functions on occasion curved away

from the overall trendline in order to fit the final data-point in a data-series). Determining the optimal range of values involves a degree of subjectivity, and thus the range is always reported together with values derived using this model. Scaling was achieved by (a) fitting third order polynomial functions to the raw (unaveraged) data at each temperature, and (b) using a Generalized Reduced Gradient Algorithm (Microsoft Solver) to minimise the least squares difference of 20 separate time points derived from the third order polynomial functions. Scaling the data acquired at different temperatures in this manner yields relative rates of reaction ($k^{(rel)}$), which in our case we chose to normalise to the mid-temperature point (110 °C).

Examples of the "overlay plots" produced using the 'model-free' approach for THAA and FAA Asx racemization are shown in Fig. 14a. Values for $k^{(rel)}$ estimated using the 'model-free' approach are reported in Table A6 of the supplementary material, along with the D/L range over which they were calculated, and the effective activation energies derived using all temperatures (E_a 26–140 °C), and derived using just the experimental high-temperatures (E_a 80–140 °C). An example of an Arrhenius plot for THAA Asx is shown in Fig. 14b. The effective activation energy estimated using the relative rate constants for just the experimental data (E_a 80–140 °C) was also applied to calculate $k^{(rel)exp26}$ (as was done previously for the RFOK and power-transformation models).

The effective activation energy (E_a 26–140 °C) values derived using the 'model-free' approach for Asx, Glx, Ala and Phe, lie between a relatively narrow range of 125–132 kJ mol^{-1} (Table 2). We also truncated the range over which the 'model-free' method was applied to only those D/L values observed at all three of the high-temperatures (80 °C, 110 °C and 140 °C). This provided an upper D/L limit of 0.52 (Asx), 0.3 (Glx), 0.53 (Ala) and 0.38 (Phe), a similar D/L range to the "truncated" data sets used for the power transformations. In all cases, implementing upper D/L limits resulted in very small changes to E_a values (<1 kJ mol^{-1}), which would not impact on any subsequent conclusions. If the data-range is further truncated to only include D/L values overlapping for the entire temperature range (26–140 °C), the maximum change in E_a values is ~3 kJ mol^{-1} (for Asx). When the amino acids tested here are ordered according to increasing temperature sensitivity, the 'model-free', RFOK slow component, and power-transformation approaches provide the same relative order: Phe, Ala, Asx, Glx. The fast linear component of the RFOK model approach produces a different order, though Glx again has an E_a > Asx. However, for the THAA fraction of all the amino acids considered, the E_a values derived using the 'model-free' approach are higher than those acquired using the other conventional approaches (with the exception of the E_a derived for Phe from the fast linear component of the RFOK model, and that derived for Glx using the power transformation with the truncated data-set). Using the same 'model-free' approach, Demarchi et al., 2013a ; Demarchi et al., 2013b also found Glx to be the most temperature sensitive amino acid, followed by Asx, but in contrast to this study, found Phe to have a higher E_a than Ala.

The k^{rel} values acquired from the 'model-free' approach, using just the experimental data, yield an estimated effective E_a of 134 kJ mol^{-1} for THAA Asx racemisation in intra-crystalline *Porites*. Including field rates (26 °C data) provides a similar, though slightly lower (and presumably more accurate) estimate of about 131 kJ mol^{-1} (Table 2). This estimate lies within the range, though towards the higher end of, previously reported values for other biominerals: ~123 kJ mol^{-1} in ostracodes (Kaufman, 2000), ~132 kJ mol^{-1} in foraminifera (Kaufman, 2006), ~126 kJ mol^{-1} for the bivalve molluscs *Hiatella* and *Mya* (Manley et al., 2000), and between ~110 and 125 kJ mol^{-1} for land snails (Goodfriend and Meyer, 1991). Using this same 'model-free' approach, a slightly higher E_a value of 137 kJ mol^{-1} was reported for *Patella* (Demarchi et al., 2013a), while a slightly lower value (125 kJ mol^{-1}) was reported for ratite eggshell (Crisp et al., 2013).

For the amino acids tested here, although none of the models are perfect, the 'model-free' approach appears to provide the most reliable estimates of the observed rates of racemization in the 'naturally aged' coral (Fig. 13 and comparison of $k^{(rel)exp26}$ and $k^{(rel)26}$ in Table 2). Although not

generally the case for the other models examined here, the 'model-free' approach performs well for THAA Phe, THAA Ala, FAA Asx and FAA Glx, despite the greater variability associated with this data. The unexpected exception is THAA Asx D/L which has greater disparity of $k^{(rel)exp26}$ and $k^{(rel)26}$. This result is surprising given that the 'model-free' approach provides reasonably precise estimates of $k^{(rel)26}$ for amino acids displaying much greater variability than the well constrained THAA Asx data. It is possible that relatively large differences in the pattern of degradation at higher temperatures for this amino acid (e.g. Section 3.6) preclude accurate extrapolation of rates from high to low temperatures.

The same 'model-free' approach was applied to derive k^{rel} and, subsequently, E_a values for hydrolysis using %FAA values (e.g. Fig. 14a for Asx, and Table A7 of the supplementary material). Values for k^{rel} and E_a were calculated for Asx, Glx, Ser, Ala and Leu hydrolysis, using both the entire temperature range (E_a 26–140 °C) and just the experimental high-temperature data (E_a 80–140 °C) (Table 3). As with the racemization data, the 'model-free' approach was additionally tested using (a) only the range of %FAA values that were observed at all three high-temperature experiments, and (b) only the range of %FAA values observed over the entire range of temperatures (26–140 °C). In neither case did this make a significant difference to the estimated hydrolysis E_a values of any of the amino acids tested (with a maximum change of 0.7 kJ mol^{-1}). Similarly, applying upper-limits of %FAA values equivalent to the [bound]/[total] limits used in the IFOK model did not influence the E_a values significantly (<1 kJ mol^{-1}).

As was the case for racemization, the effective E_a values derived for hydrolysis (using the entire temperature range of 26–140 °C) lie in a relatively narrow range: 112–116 kJ mol^{-1}(Table 3). The E_a values for Asx and Glx are only 1 kJ mol^{-1} higher than the estimates made using the IFOK model (Section 3.7.2), though the value for Ala is ~10 kJ mol^{-1} higher. These E_a values also bracket estimates derived using both heated and (^{14}C dated) fossil ostrich eggshell for Leu hydrolysis (~114 kJ mol^{-1}; Miller et al., 1992); similar values were also estimated by Collins and Riley (2000) from well-dated foraminifera (King, 1980). These estimates are higher than activation energies calculated under ideal conditions (dipeptides heated in the laboratory; E_a 83–99 kJ mol^{-1}e.g. Kriausakul and Mitterer, 1980 ; Qian et al., 1993) probably due to the effect of protein structure on the hydrolysis rates: estimated E_a's are elevated because they also include rate changes associated with protein denaturation, hydrolysis being faster in disordered peptide chains. An additional factor will be the rate of decomposition of free amino acids. Hydrolysis rates are estimated from the rate of increase in %FAA, but this apparent rate may vary between temperatures if there are differences in the temperature dependence of hydrolysis and decomposition.

As with the racemization data, the high-temperature (80 °C, 110 °C and 140 °C) $k^{(rel)}$values for hydrolysis were used to estimate the E_a of hydrolysis, which was then used to predict the rate constant for hydrolysis at 26 °C ($k^{(rel)exp26}$). The value of $k^{(rel)exp26}$ for hydrolysis was subsequently compared to the "observed" rate constant for hydrolysis calculated from just the 'naturally aged' *Porites* samples ($k^{(rel)26}$). For Asx, Glx and Ala (the amino acids for which both racemization and hydrolysis were examined using the 'model-free' approach), larger discrepancies are apparent between $k^{(rel)26}$ and $k^{(rel)exp26}$, for hydrolysis than for racemization (Fig. 13). With the exception of Leu, when the entire range of k^{rel} values (incorporating the 'naturally aged' coral) are used to calculate an effective E_a for hydrolysis, the values derived are lower than when just the experimental (80–140 °C) data are applied. It is difficult to identify the true cause of discrepancies between E_a values calculated using the different temperature ranges (i.e. with and without the 'naturally aged' coral). Limitations in our ability to measure and model the reaction accurately, and differences in the temperature sensitivities of underlying reactions, are both likely to be, at least in some part, accountable. It is interesting that the IFOK model predicted the rate of observed Asx hydrolysis in

the 'naturally aged' coral much more accurately than the 'model-free' approach, though deviation from IFOK in the more degraded samples (such as the highest time points at 110 °C), indicates that this model is not applicable over the entire reaction.

Irrespective of the temperature-range applied, for those amino acids for which comparisons can be made (Asx, Glx, and Ala), the E_a value calculated for hydrolysis using the 'model-free' approach falls significantly below the E_a value for racemization (Fig. 14c, Table 2 ; Table 3). This is also true when IFOK (hydrolysis) and RFOK (racemization) were applied to estimate E_a values. Using the same 'model-free' approach, Demarchi et al. (2013a) reported similar results for a broad range of amino acids (Asx, Glx, Ser, Ala, Val, Phe, Leu and Ile) in *Patella vulgata*. The net effect of the offset in temperature sensitivity is that as temperature increases the rate of racemization rises relatively faster than the rate of hydrolysis.

Differences in the temperature sensitivities of hydrolysis and racemization could account for differences in degradation patterns observed at different temperatures (e.g. Fig. 12c). At low temperatures, FAA generation is high relative to racemization and therefore, we observe a high %FAA compared to THAA Asx D/L. At high temperatures, the rate of racemization is increased relative to FAA generation and therefore, we observe a lower %FAA for a given degree of THAA Asx D/L. Differences in degradation patterns between high and low temperatures are not anticipated to be the same in all substrates or amino acids, because of differences in the relative rates of hydrolysis (a function of the richness of labile peptide bonds) and denaturation (influenced by higher order structure and thermal stability). Demarchi et al. (2013a) and Crisp et al. (2013) observe broadly similar patterns in *Patella* shell and ostrich eggshell respectively. However, differences between these three studies suggest that the relative rate differences between hydrolysis and racemization are more evident in molluscs and corals, in which the OM appears to be comprised of more polar (and therefore possibly more flexible) intra-crystalline proteins (e.g. Mann et al., 2012), than eggshell (e.g. Reyes-Grajeda et al., 2004 ; Freeman et al., 2010).

Racemization will occur either in denatured stretches (for Asx & Ser; Geiger and Clarke, 1987 ; Takahashi et al., 2010) or at N-terminal (all other amino acids) positions (Kriausakul and Mitterer, 1978; Kriausakul and Mitterer, 1980 ; Moir and Crawford, 1988) of degrading proteins. In the case of Asx, a decrease in the rate of hydrolysis relative to racemization at higher temperatures will mean increased opportunity for Asx to racemize via (bound) succinimidyl residues prior to hydrolysis to free amino acids. We suggest that this may account for the decreasing differences between the extent of AAR in the FAA v.s. THAA pools observed in Fig. 12b at progressively higher temperatures.

The marked difference in E_a between racemization and hydrolysis observed in this study for Asx, Glx and Ala in *Porites* coral invalidates one of the key assumptions associated with extrapolation of racemization kinetics from heating-experiments; namely, that the underlying reactions that contribute to the observed rate of racemization of these amino acids, do not differ significantly in their temperature sensitivity. In this case, the lower temperature-sensitivity of hydrolysis in these amino acids means that it could become the rate-limiting reaction at high-temperatures, potentially resulting in "unexpectedly" low k for racemization. However, this may only be the case for the amino acids (Asx, Glx, and Ala) examined in this study, and potentially, only apply to the *Porites* coral biomineral.

In contrast, Laabs and Kaufman (2003) demonstrated that over the D/L range tested, the relative rates of racemization for Asx and Glx in heated (110 °C and 140 °C) mollusc genera appear concordant with those of unheated Pleistocene samples. Similarly, Miller et al. (2000) observed matching patterns of Ile epimerization in heated (143 °C) modern and fossil *Dromaius* eggshell, despite the samples possessing very different thermal histories. Miller et al. (2000) concluded that

underlying reactions must, therefore, have effectively the same E_a as Ile epimerization. Given that Ile does not epimerize when internally bound within a peptide chain (Mitterer and Kriausakul, 1984), differences in A/I values between the FAA and THAA fractions of heated modern and fossil eggshell will be related to Ile hydrolysis (Miller et al., 2000). Unlike our results for Asx (Fig. 12b), Miller et al. (2000) found that the relationship between Ile THAA A/I and Ile FAA A/I did not vary systematically with temperature, providing further evidence of the similarity between Ile hydrolysis and racemization E_a in *Dromaius* eggshell. The E_a reported by Miller et al. (1992) for Leu hydrolysis ($\sim$114 kJ mol^{-1}) however, may to some extent mask the additional temperature input required to denature the rigid eggshell protein (Freeman et al., 2010). The low Ile concentration (Fig. 3) and poor resolution of D and L enantiomers of Ile in the coral OM, prevents any meaningful comparison between Miller et al. (2000) and our study.

3.8. Dynamic modelling of racemization kinetics

In this study we have explored the potential for extrapolating high temperature experiments to the lower temperatures to which fossils are naturally exposed in the environment. Our data clearly shows that protein degradation does not always follow the same pathways at ambient and elevated temperatures for the intra-crystalline protein of *Porites*. However, whilst acknowledging that the effective Arrhenius parameters calculated using such methods may therefore be imprecise, they should provide estimates which are approximately (in the same order of magnitude) correct. In this study, by constraining the experimental data with well-dated 'naturally aged' coral skeleton that has remained at an almost constant temperature, we reduce the errors associated with estimates of the temperature-sensitivity of degradation reactions. We suggest that a productive approach is to use the effective Arrhenius parameters determined in studies such as this to provide the basis for dynamic models that simulate the racemization reaction. A schematic model for Asx racemization is shown in Fig. 15. Multiple reactions (such as free, terminal and bound racemization, hydrolysis and decomposition) all contribute to the observed THAA and FAA DL ratio, and each of these reactions will occur at a different rate, determined by variables such as temperature, water availability, and protein sequence and structure. By factoring in experimentally derived Arrhenius parameters (k, E_a, $\ln(A)$) for these underlying-reactions, we can begin to examine how each component influences the behaviour of the whole system. The experimentally derived values enable an initially "sensible" output from the simulation that would otherwise be extremely difficult to achieve. These values can subsequently be refined to better simulate the expected racemization patterns. In order for this modelling approach to be successful, it is important that an intra-crystalline (closed-system) fraction is analysed; the kinetics will ultimately be tractable, as products of the reaction (e.g. FAA) are retained (Collins and Riley, 2000).
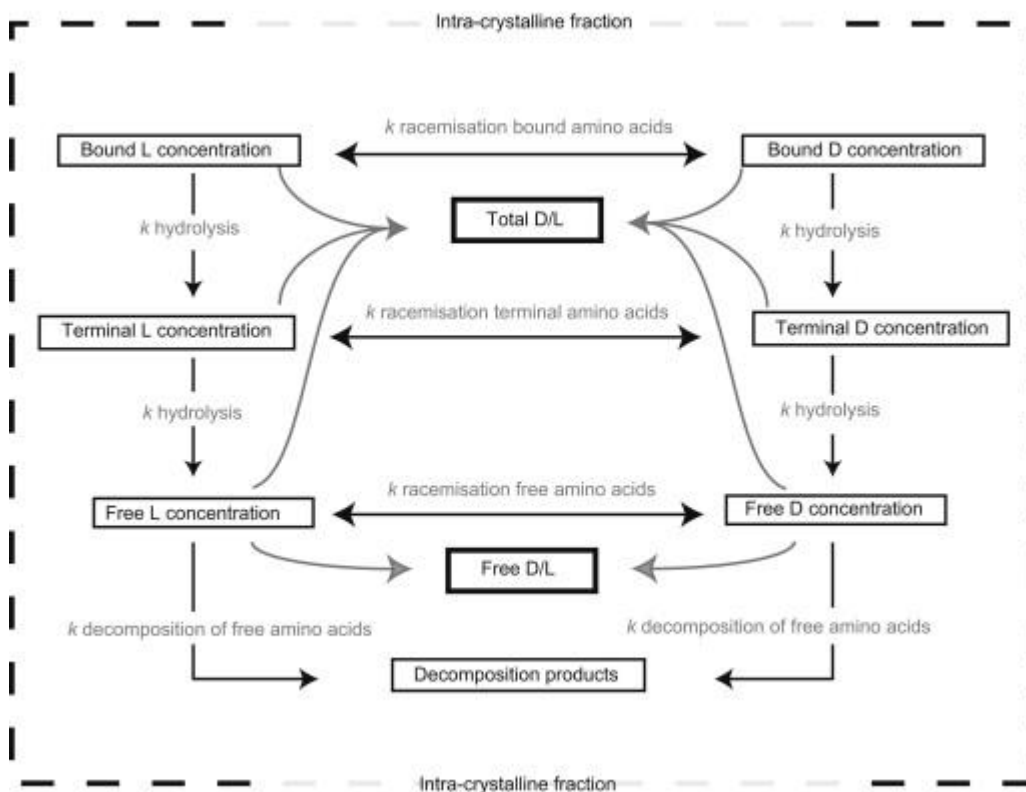
Fig. 15.

Schematic representation of aspartic acid racemization. Though an oversimplification, simultaneously solving the multiple equations incorporated into the model may provide the best approach to understanding the kinetics of racemization. Each of the reactions should have an individual rate constant, k, which is equal to; $A * \exp(E_a/(R * T))$, where A = the pre-exponential factor, E_a = the activation energy, R = the universal gas constant (8.314 J mol^{-1}), T = the absolute temperature (in K). Variables, such as water availability and peptide bond strength (which influence hydrolysis rate) and temperature will influence k for each reaction. Asx is atypical in that it can racemize whilst bound; this is thought to occur via the formation of a succinimide intermediate (Geiger and Clarke, 1987). Potential decomposition products include fumaric acid (+NH$_3$), which is formed via reversible deamination, and Ala, formed via decarboxylation. This model represents reactions taking place in the intra-crystalline fraction; the products of degradation are retained, while contaminants are excluded.

Figure options

4. Conclusions

Estimates of the rate of reactions in amino geochronology are necessarily derived through high-temperature experiments to examine reaction pathways. However, the patterns of racemization and hydrolysis are in reality complex, and furthermore, heating experiments conducted at lower temperatures are unable to run sufficiently long to fully cover the pattern of kinetics. The combined effect of these two factors is that higher temperature model fits, which include more latter stage data, may tend to underestimate rates relative to lower temperature studies (which only encompass the early stages of diagenesis).

To examine the validity of extrapolating kinetic parameters from high-temperature experiments, to the lower temperatures experiences *in vivo*, we compared the behaviour of protein degradation in the intra-crystalline organic matrix of heated (80 °C, 110 °C, and 140 °C) massive *Porites* sp. coral to that directly measured in skeleton from colonies growing at ~26 °C and deposited over the last five centuries. We introduce a 'model-free' technique, fitting relative rates using a numerical approach, and assess this against conventional methods of deriving kinetic parameters. Our estimates are relatively good predictors of racemization rates (for both the THAA and FAA

fractions of specified amino acids) observed in a well-dated geological system. However, this approach generally overestimates the activation energy of hydrolysis; the most probable explanation is that at the higher temperatures used in the experimental study all the proteins are denatured, yet in the 'naturally aged' samples, persisting conformation is lowering hydrolysis rates. The E_a for Asx and Glx hydrolysis is better predicted by the IFOK model (though only the very earliest stages of degradation were modelled for Glx, due to rapid deviation away from IFOK).

It is relatively unlikely that the various reactions contributing to racemization all have the same activation energies (and hence temperature dependence) although this is the assumption when extrapolating from high-temperature experiments. The higher temperature sensitivity of racemization compared to hydrolysis, demonstrated in this study for all three amino acids for which reliable data was acquired (Asx, Glx and Ala), will cause more rapid generation of free amino acids relative to racemisation at lower temperatures, than in experimental heating studies. If the system was not closed, this would further complicate interpretation. For example, diffusion is a much less temperature sensitive process than racemization or hydrolysis (see Collins and Riley, 2000; and references therein), and therefore the increase in the rate of diffusive loss of (highly racemized) free amino acids at higher temperatures, is likely to be relatively small, compared to the corresponding increase in rates of hydrolysis and racemization.

Observed differences in degradation pathways of Asx, Glx, and Ala at different temperatures have now been found in various biominerals, limiting the applicability of high-temperature experiments for these amino acids (although heating at lower temperatures may better replicate degradation patterns observed in fossil samples). We suggest that dynamic modelling of racemization (which can utilize the approximate effective Arrhenius parameters acquired from heating-experiments) represents a logical progression in our attempts to understand the kinetics of racemization.

Acknowledgements

Bada, J.L., 1972. The dating of fossil bones using the racemization of isoleucine. Earth and Planetary Science Letters 15, 223e231.

Bada, J.L., 1984. Racemisation of amino acids. In: Barrett, G.C. (Ed.), Chemistry and Biochemistry of the Amino Acids. Chapman & Hall, London, pp. 399e414.

Bada, J.L., 1991. Amino acid cosmogeochemistry. Philosophical Transactions of the Royal Society of London, Series B 333, 349e358. Bada, J.L., Man, E.H., 1980. Amino acid diagenesis in deep sea drilling project cores: kinetics and mechanisms of some reactions and their applications in geochronology and in paleotemperature and heat flow determinations. EarthScience Reviews 16, 21e55.

Bada, J.L., Miller, S.L., 1968. Ammonium ion concentration in the primitive ocean. Science 159, 423e425.

Bada, J.L., Miller, S.L., 1970. The kinetics and mechanism of the reversible nonenzymatic deamination of aspartic acid. Journal of the American Chemical Society 92, 2774e2782.

Bada, J.L., Schroeder, R.A., 1972. Racemization of isoleucine in calcareous marine sediments: kinetics and mechanism. Earth and Planetary Science Letters 15,1e11.

Bada, J.L., Shou, M.Y., Man, E.H., Schroeder, R.A., 1978. Decomposition of hydroxy amino acids in foraminiferal tests: kinetics, mechanism and geochronological implications. Earth and Planetary Science Letters 41, 67e76.

Berman, A., Hanson, J., Leiserowitz, L., Koetzle, T.F., Weiner, S., Addadi, L., 1993. Biological control of crystal texture: a widespread strategy for adapting crystal properties to function. Science 259, 776e779.

Brinton, K.L.F., Bada, J.L., 1995. Comment on "Aspartic acid racemization and protein diagenesis in corals over the last 350 years" by Goodfriend, G. A., Hare, P. E., and Druffel., E. R. M. Geochimica et Cosmochimica Acta 59, 415e416.

Brooks, A.S., Hare, P.E., Kokis, J.E., Miller, G.H., Ernst, R.D., Wendorf, F., 1990. Dating Pleistocene archeological sites by protein diagenesis in ostrich eggshell. Science 248, 60e64.

Clarke, S., Murray-Wallace, C.V., 2006. Mathematical expressions used in amino acid racemisation geochronologyda review. Quaternary Geochronology 1, 261e278.

Collins, M.J., Riley, M.S., 2000. Amino acids racemization in biominerals: the impact of protein degradation and loss. In: Goodfriend, G.A., Collins, M.J., Fogel, M.L., Macko, S.A., Wehmiller, J.F. (Eds.), Perspectives in Amino Acid and Protein Geochemistry. Oxford University Press, New York, pp. 120e142.

Collins, M.J., Westbroek, P., Muyzer, G., De Leeuw, J.W., 1992. Experimental evidence for condensation reactions between sugars and proteins in carbonate skeletons. Geochimica et Cosmochimica Acta 56, 1539e1544.

Collins, M.J., Walton, D., King, A., 1998. The geochemical fate of proteins. In: Stankiewiez, B.A., Van Bergen, P.F. (Eds.), Nitrogen Containing Macromolecules in the Bio- and Geosphere. ACS Symposium Series, vol. 707, pp. 74e77.

Collins, M.J., Waite, E.R., van Duin, A.C.T., 1999. Predicting protein decomposition: the case of aspartic-acid racemization kinetics. Philosophical Transactions of the Royal Society of London, Series B 352, 51e64.

Constantz, B.,Weiner, S.,1988. Acidic macromolecules associated with the mineral phase of scleractinian coral skeletons. Journal of Experimental Zoology 248, 253e258.

Crisp, M., Demarchi, B., Collins, M.J., Penkman, K.E.H., 2013. Isolation of the intracrystalline proteins and kinetic studies in Struthio camelusfor amino acid geochronology. Quaternary Geochronology 16, 110e128.

Cuif, J.P., Dauphin, Y., Gautret, P., 1999. Compositional diversity of soluble mineralizing matrices in some recent coral skeletons compared to fine-scale growth structures of fibres: discussion of consequences for biomineralization and diagenesis. International Journal of Earth Sciences 88, 582e592.

Cuif, J.P., Dauphin, Y., Berthet, P., Jegoudez, J., 2004. Associated water and organic compounds in coral skeletons: quantitative thermogravimetry coupled to infrared absorption spectrometry. Geochemistry Geophysics Geosystems 5, 1e9.

Demarchi, B., 2009. Geochronology of coastal prehistoric environments: a new closed system approach using amino acid racemisation. Unpublished Ph.D. thesis, University of York, York, UK.

Demarchi, B., Collins, M.J., Tomiak, P.J., Davies, B.J., Penkman, K.E.H., 2013a. Intracrystalline protein diagenesis (IcPD) in Patella Vulgata. Part II: Breakdown and temperature sensitivity. Quaternary Geochronology 16, 158e172.

Demarchi, B., Rogers, K., Fa, D.A., Finlayson, C.J., Milner, N., Penkman, K.E.H., 2013b. Intra-crystalline protein diagenesis (IcPD) in Patella vulgata. Part I: Isolation and testing of the closed system. Quaternary Geochronology 16, 144e157.

Demarchi, B., Williams, M.G., Milner, N., Russell, N., Bailey, G., Penkman, K.E.H., 2011. Amino acid racemization dating of marine shells: a mound of possibilities. Quaternary International 239, 114e124.

Dunbar, R.B., Wellington, G.M., 1981. Stable isotopes in branching coral monitor seasonal temperature variation. Nature 293, 453e455. Epstein, S., Buchsbaum, R., Lowenstam, H.A., Urey, H.C., 1953. Revised carbonatewater isotopic temperature scale. Bulletin of the Geological Society of America 64, 1315e1326.

Freeman, C.L., Harding, J.H., Quigley, D., Rodger, P.M., 2010. Structural control of crystal nuclei by an eggshell protein. Angewandte Chemie-International Edition 49, 5135e5137.

Gaffey, S.J., 1988. Water in skeletal carbonates. Journal of Sedimentary Petrology 58, 397e414.

Gaffey, S.J., Bronnimann, C.E., 1993. Effects of bleaching on organic and mineral phases in biogenic carbonates. Journal of Sedimentary Petrology 63, 752e754.

Geiger, T., Clarke, S., 1987. Deamidation, isomerization, and racemization at asparaginyl and aspartyl residues in peptides. The Journal of Biological Chemistry 262, 785e794.

Goodfriend, G.A., 1991. Patterns of racemization and epimerization of amino acids in land snail shells over the course of the Holocene. Geochimica et Cosmochimica Acta 55, 293e302.

Goodfriend, G.A., 1992. Rapid racemization of aspartic acid in mollusc shells and potential for dating over recent centuries. Nature 357, 399e401.

Goodfriend, G.A., Meyer, V.R., 1991. A comparative study of the kinetics of amino acid racemization/epimerization in fossil and modern mollusk shells. Geochimica et Cosmochimica Acta 55, 3355e3367.

Goodfriend, G.A., Hare, P.E., Druffel, E.R.M., 1992. Aspartic acid racemization and protein diagenesis in corals over the last 350 years. Geochimica et Cosmochimica Acta 56, 3847e3850.

Goodfriend, G.A., Kashgarian, M., Harasewych, M.G., 1995. Use of aspartic acid racemization and post-bomb 14C to reconstruct growth rate and longevity of the deep-water slit shell Entemnotrochus adansonianus.

Geochimica et Cosmochimica Acta 59, 1125e1129. Goodfriend, G.A., Brigham-Grette, J., Miller, G.H., 1996. Enhanced age resolution of the marine Quaternary record in the Arctic using aspartic acid racemization dating of bivalve shells. Quaternary Research 45, 176e187.

Gotliv, B., Addadi, L., Weiner, S., 2003. Mollusk shell acidic proteins: in search of individual functions. Chembiochem 4, 522e529.

Hendy, E.J., Gagan, M.K., Alibert, C.A., McCulloch, M.T., Lough, J.M., Isdale, P.J., 2002. Abrupt decrease in tropical Pacific sea surface salinity at end of Little Ice Age. Science 295, 1511e1514.

Hendy, E.J., Gagan, M.K., Lough, J.M., 2003. Chronological control of coral records using luminescent lines and evidence for non-stationary ENSO teleconnections in northeast Australia. The Holocene 13, 187e199.

Hendy, E.J., Tomiak, P.J., Collins, M.J., Hellstrom, J., Tudhope, A.W., Lough, J.M., Penkman, K.E.H., 2012. Assessing amino acid racemization variability in coral intra-crystalline protein for geochronological applications. Geochimica et Cosmochimica Acta 86, 338e353.

Hill, R.L., 1965. Hydrolysis of proteins. In: Anfinsen, C.B.J., Anson, M.L., Edsall, J.T., Richards, F.M. (Eds.), Advances in Protein Geochemistry. Academic Press, New York, pp. 37e107.

Hoering, T.C., 1973. A comparison of melanoidin and humic acid. Carnegie Institution of Washington Yearbook, vol. 72, pp. 682e690.

Ingalls, A.E., Lee, C., Druffel, E.R.M., 2003. Preservation of organic matter in moundforming coral skeletons. Geochimica et Cosmochimica Acta 67, 2827e2841.

Kaufman, D.S., 2000. Amino acid racemization in ostracodes. In: Goodfriend, G.A., Collins, M.J., Fogel, M.L., Macko, S.A., Wehmiller, J.F. (Eds.), Perspectives in Amino Acid and Protein Geochemistry. Oxford University Press, New York, pp. 145e160.

Kaufman, D.S., 2003. Amino acid paleothermometry of Quaternary ostracodes from the Bonneville Basin, Utah. Quaternary Science Reviews 22, 899e914.

Kaufman, D.S., 2006. Temperature sensitivity of aspartic and glutamic acid racemization in the foraminifera Pulleniatina. Quaternary Geochronology 1, 188e207.

Kaufman, D.S., Manley, W.F., 1998. A new procedure for determining DL amino acid ratios in fossils using reverse phase liquid chromatography. Quaternary Geochronology 17, 987e1000.

Kaufman, D.S., Miller, G.H., 1995. Isoleucine epimerization and amino acid composition in molecular-weight separations of Pleistocene Genyornis eggshell. Geochimica et Cosmochimica Acta 59, 2757e2765.

Kaufman, D.S., Sejrup, H.P., 1995. Isoleucine epimerization in the high-molecularweight fraction of Pleistocene Arctica. Quaternary Science Reviews 14, 337e350.

Kimber, R.W.L., Griffin, C.V., 1987. Further evidence of the complexity of the racemization process in fossil shells with implications for amino acid racemization dating. Geochimica et Cosmochimica Acta 51, 839e846.

Kimber, R.W.L., Hare, P.E., 1992. Wide range of racemization of amino acids in peptides from human fossil bone and its implications for amino acid racemization dating. Geochimica et Cosmochimica Acta 56, 739e743.

King Jr., K., 1980. Applications of amino acid biogeochemistry for marine sediments. In: Hare, P.E., Hoering, T.C., King Jr., K. (Eds.), Biogeochemistry of Amino Acids. Wiley, New York, pp. 377e391. King Jr., K., Hare, P.E., 1972. Amino acid composition of the test as a taxonomic character for living and fossil planktonic Foraminifera. Micropaleontology 18, 285e293.

Kosnik, M.A., Kaufman, D.S., 2008. Identifying outliers and assessing the accuracy of amino acid racemization measurements for geochronology: II. Data screening. Quaternary Geochronology 3, 328e341.

Kriausakul, N., Mitterer, R.M., 1978. Isoleucine epimerization in peptides and proteins: kinetic factors and application to fossil proteins. Science 201, 1011e1014.

Kriausakul, N., Mitterer, R.M., 1980. Comparison of isoleucine epimerization in a model dipeptide and fossil protein. Geochimica et Cosmochimica Acta 44, 753e758.

Kvenvolden, K.A., Peterson, E., Wehmiller, J.F., Hare, P.E., 1973. Racemization of amino acids in marine sediments determined by gas chromatography. Geochimica et Cosmochimica Acta 37, 2215e2225.

Laabs, B.J.C., Kaufman, D.S., 2003. Quaternary highstands in Bear Lake Valley, Utah and Idaho. Geological Society of America Bulletin 115, 463e478. Land, L.S., Lang, J.C., Barnes, D.J., 1975. Extension rate: a primary control on the isotopic composition of West Indian (Jamaican) Scleractinian reef coral skeletons. Marine Biology 33, 221e233.

Manley, W.F., Miller, G.H., Czywczynski, J., 2000. Kinetics of aspartic acid racemization in Mya and Hiatella: modeling age and paleotemperature of high-latitude quaternary mollusks. In: Goodfriend, G.A., Collins, M.J., Fogel, M.L., Macko, S.A., Wehmiller, J.F. (Eds.), Perspectives in Amino Acid and Protein Geochemistry. Oxford University Press, New York, pp. 202e218.

Mann, K., Edsinger-Gonzales, E., Mann, M., 2012. In-depth proteomic analysis of a mollusc shell: acid-soluble and acid-insoluble matrix of the limpet Lottia gigantea. Proteome Science 10. http://dx.doi.org/10.1186/1477-5956-10-28.

Mansur, H.S., Mansur, A.A.P., Marivalda, M.P., 2005. XRD, SEM/EDX and FTIR characterization of Brazilian natural coral. Key Engineering Materials 284e286, 43e46.

Mass, T., Brickner, I., Hendy, E.J., Genin, A., 2011. Enduring physiological and reproductive benefits of enhanced flow for a stony coral. Limnology and Oceanography 56, 2176e2188.

Masters, P.M., Bada, J.L., 1977. Racemization of isoleucine in fossil molluscs from Indian middens and interglacial terraces in southern California. Earth and Planetary Science Letters 37, 173e183.

Masters, P.A., Bada, J.L., 1978. Amino acid racemization dating of bone and shell. In: Carter, G.F. (Ed.), Archaeological Chemistry II. American Chemical Society, Washington, D.C., pp. 117e138.

McCoy, W.D., 1987. The precision of amino acid geochronology and paleothermometry. Quaternary Science Reviews 6, 43e54. Miller, G.H., Brigham-Grette, 1989. Amino acid geochronology: resolution and precision in carbonate fossils. Quaternary International 1, 111e128.

Miller, G.H., Wendorf, F., Ernst, R., Schild, R., Close, A.E., Friedman, I., Schwarcz, H.P., 1991. Dating lacustrine episodes in the eastern Sahara by the epimerization of isoleucine in ostrich eggshells. Palaeogeography, Palaeoclimatology, Palaeoecology 84, 175e189.

Miller, G.H., Beaumont, P.B., Jull, A.J.T., Johnson, B., 1992. Pleistocene geochronology and palaeothermometry from protein diagenesis in ostrich eggshells: implications for the evolution of modern humans. Philosophical Transactions of the Royal Society of London, Series B 337, 149e157.

Miller, G.H., Beaumont, P.B., Deacon, H.J., Brooks, A.S., Hare, P.E., Jull, A.J.T., 1999. Earliest modern humans in southern Africa dated by isoleucine epimerization in ostrich eggshell. Quaternary Science Reviews 18, 1537e1548.

Miller, G.H., Hart, C.P., Roark, B., Johnson, B.J., 2000. Isoleucine epimerization in eggshells of the flightless Australian birds Genyornis and Dromaius. In: Goodfriend, G.A., Collins, M.J., Fogel, M.L., Macko, S.A., Wehmiller, J.F. (Eds.), Perspectives in Amino Acid and Protein Geochemistry. Oxford University Press, New York, pp. 161e181.

Mitterer, R.M., 1975. Ages and diagenetic temperatures of Pleistocene deposits of Florida based on Isoleucine epimerization in Mercenaria. Earth and Planetary Science Letters 28, 275e282.

Mitterer, R.M., 1978. Amino acid composition and metal binding capability of the skeletal protein of corals. Bulletin of Marine Science 28, 173e180.

Mitterer, R.M., Kriausakul, N., 1984. Comparison of rates and degrees of isoleucine epimerization in dipeptides and tripeptides. Organic Geochemistry 7, 91e98.

Mitterer, R.M., Kriausakul, N., 1989. Calculation of amino acid racemization ages based on apparent parabolic kinetics. Quaternary Science Reviews 8, 353e357.

Moir, M.E., Crawford, R.J., 1988. Model studies of competing hydrolysis and epimerization of some tetrapeptides of interest in amino acid racemization studies in geochronology. Canadian Journal of Chemistry 66, 2903e2913.

Orem, C.A., Kaufman, D.S., 2011. Effects of basic pH on amino acid racemization and leaching in freshwater mollusk shell. Quaternary Geochronology 6, 233e245.

Penkman, K.E.H., Preece, R.C., Keen, D.H., Maddy, D., Schreve, D.C., Collins, M.J., 2007. Testing the aminostratigraphy of fluvial archives: the evidence from intra-crystalline proteins within freshwater shells. Quaternary Science Reviews 26, 2958e2969.

Penkman, K.E.H., Kaufman, D.S., Maddy, D., Collins, M.J., 2008a. Closed-system behaviour of the intra-crystalline fraction of amino acids in mollusc shells. Quaternary Geochronology 3, 2e25.

Penkman, K.E.H., Preece, R.C., Keen, D.H., Collins, M.J., 2008b. British Aggregates: an Improved Chronology Using Amino Acid Racemization and Degradation of Intra-crystalline Amino Acids (IcPD). English Heritage Research Department Reports Series 6.

Penkman, K.E.H., Preece, R.C., Keen, D.H., Collins, M.J., 2010. Amino acid geochronology of the type Cromerian of West Runton, Norfolk, UK. Quaternary International 228, 25e37.

Penkman, K.E.H., Preece, R.C., Bridgland, D.R., Keen, D.H., Meijer, T., Parfitt, S.A., White, T.S., Collins, M.J., 2011. A chronological framework for the British Quaternary based on Bithynia opercula. Nature 476, 446e449.

Pingitore, N.E., Fretzdorf, S.B., Seitz, B.P., Estrada, L.Y., Borrego, P.M., Crawford, G.M., Love, K., 1993. Dissolution kinetics of CaCO3 in common laboratory solvents. Journal of Sedimentary Petrology 63, 641e645.

Puverel, S., Tambutté, E., Pereira-Mouriès, L., Zoccola, D., Allemand, D., Tambutté, S., 2005. Soluble organic matrix of two Scleractinian corals: partial and comparative analysis. Comparative Biochemistry and Physiology, Part B 141, 480e487.

Qian, Y.R., Engle, M.H., Macko, S.A., Carpenter, S., Deming, J.W., 1993. Kinetics of peptide hydrolysis and amino acid decomposition at high temperature. Geochimica et Cosmochimica Acta 57, 3281e3293.

Qian, Y.R., Engel, M.H., Goodfriend, G.A., Macko, S.A., 1995. Abundance and stable carbon isotope composition of amino acids in molecular weight fractions of fossil and artificially aged mollusc shells. Geochimica et Cosmochimica Acta 59, 1113e1124.

Rafalska, J.K., Engel, M.H., Lanier, W.P., 1991. Retardation of racemization rates of amino acids incorporated into melanoidins. Geochimica et Cosmochimica Acta 55, 3669e3675.

Rahman, M.A., Oomori, T., 2008. Aspartic acid-rich proteins in insoluble organic matrix play a key role in the growth of calcitic sclerites in Alcyonarian coral. Chinese Journal of Biotechnology 24, 2127e2128.

Reyes-Grajeda, J.P., Moreno, A., Romero, A., 2004. Crystal structure of Ovocleidin-17, a major protein of the calcified Gallus gallus eggshell e implications in the calcite mineral growth pattern. Journal of Biological Chemistry 279, 40876e40881.

Reynolds, R.W., Rayner, N.A., Smith, T.M., Stokes, D.C., Wang, W., 2002. An improved in situ and satellite SST analysis for climate. Journal of Climate 15, 1609e1625.

Roof, S., 1997. Comparison of isoleucine epimerization and leaching potential in the molluskan genera Astarte, Macoma, and Mya. Geochimica et Cosmochimica Acta 61, 5325e5333.

Schroeder, R.A., Bada, J.L., 1976. A review of the geochemical applications of the amino acid racemization reaction. Earth-Science Reviews 12, 347e391.

Schultz, J., Allison, H., Grice, M., 1962. Specificity of the cleavage of proteins by dilute acid. I. Release of aspartic acid from insulin, ribonuclease, and glucagon. Biochemistry 1, 694e698.

Smith, G.G., Reddy, G.V., 1989. Effect of the side chain on the racemization of amino acids in aqueous solution. Journal of Organic Geochemistry 54, 4529e4535.

Sykes, G.A., Collins, M.J., Walton, D.I., 1995. The significance of a geochemically isolated intracrystalline organic fraction within biominerals. Organic Geochemistry 23, 1059e1065.

Takahashi, O., Kobayashi, K., Oda, A., 2010. Computational insight into the mechanism of serine residue racemization. Chemistry and Biodiversity 7, 1625e1629.

Towe, K.M., 1980. Preserved organic ultrastructure: an unreliable indicator for Paleozoic amino acid biogeochemistry. In: Hare, P.E., Hoering, T.C., King, K.J. (Eds.), The Biogeochemistry of Amino Acids. Wiley, New York, pp. 65e74.

Vallentyne, J.R., 1964. Biogeochemistry of organic matter e II Thermal reaction kinetics and transformation products of amino compounds. Geochimica et Cosmochimica Acta 28, 157e188.

Waite, E.R., Collins, M.J., 2000. The interpretation of aspartic acid racemization of dentine proteins. In: Goodfriend, G.A., Collins, M.J., Fogel, M.L., Macko, S.A., Wehmiller, J.F. (Eds.), Perspectives in Amino Acid and Protein Geochemistry. Oxford University Press, New York, pp. 182e194.

Walton, D., 1998. Degradation of intracrystalline proteins and amino acids in fossil brachiopods. Organic Geochemistry 28, 389e410.

Wehmiller, J.F., 1977. Amino acid studies of the Del Mar, California, midden site: apparent rate constants, ground temperature models, and chronological implications. Earth and Planetary Science Letters 37, 184e196.

Wehmiller, J.F., 1980. Intergeneric differences in apparent racemization kinetics in molluscs and foraminifera: implications for models of diagenetic racemization. In: Hare, P.E., Hoering, T.C., King Jr., K. (Eds.), Biogeochemistry of Amino Acids. Wiley, New York, pp. 341e356.

Wehmiller, J.F., 1993. Applications of organic geochemistry for Quaternary research: aminostratigraphy and aminochronology. In: Engel, M.H., Macko, S.A. (Eds.), Organic Geochemistry. Plenum Press, New York, pp. 755e783.

Wehmiller, J.F., Hare, P.E., 1971. Racemization of amino acids in marine sediments. Science 173, 907e911.

Wehmiller, J.F., Hare, P.E., Kujala, G.A., 1976. Amino acids in fossil corals: racemization (epimerization) reactions and their implications for diagenetic models and geochronological studies. Geochimica et Cosmochimica Acta 40, 763e776.

Wehmiller, J.F., Belknap, D.F., 1978. Alternative kinetic models for the interpretation of amino acid enantiomeric ratios in Pleistocene molluscs: examples from California, Washington, and Florida. Quaternary Research 9, 330e348.

Wehmiller, J.F., Miller, G.H., 2000. Aminostratigraphic dating methods in Quaternary geology. In: Noller, J.S., Sowers, J.M., Lettis, W.R. (Eds.), Quaternary Geochronology: Methods and Applications. American Geophysical Union, Washington, DC, pp. 187e222.

Weiner, S., 1979. Aspartic acid-rich proteins: major components of the soluble organic matrix of mollusk shells. Calcified Tissue International 29, 163e167.

Westaway, R., 2009. Calibration of decomposition of serine to alanine in Bithynia opercula as a quantitative dating technique for Middle and Late Pleistocene sites in Britain. Quaternary Geochronology 4, 241e259.

Young, S.D., 1971. Organic material from scleractinian coral skeletonsdI. Variation in composition between several species. Comparative Biochemistry and Physiology, Part B, 113e120.